# The roles of dystrophin and dystrobrevin : in synaptic signaling in drosophila

Potikanond, S.

# CHAPTER 3.1

## A Postsynaptic DGC/Rho-GTPase Pathway likely acting through CaMKII Controls the Homeostatic Endpoint at the *Drosophila* NMJ

# A Postsynaptic Dystrophin Glycoprotein Complex/Rho-GTPase Pathway likely acting through CaMKII Controls the Homeostatic Endpoint at the *Drosophila* Neuromuscular Junction

**Saranyapin Potikanond, Gonneke S. K. Pilgram, Anja W.M. de Jong, Lee G. Fradkin* and Jasprina N. Noordermeer***

Laboratory of Developmental Neurobiology, Department of Molecular Cell Biology, Leiden University Medical Center, Einthovenweg 20, P.O. Box 9600, 2300 RC Leiden, The Netherlands

*to whom correspondence should be addressed. Email: L.G.Fradkin@lumc.nl and J.N.Noordermeer@lumc.nl

Keywords (10): *Dystrobrevin*, *Dystrophin*, *cdc42*, *CaMKII*, Rho-GTPase, Rho-GAP, neuromuscular junction, synaptic homeostasis, retrograde signaling, *Drosophila*

## Abstract

Neurotransmitter release levels are controlled during growth to ensure proper synaptic function. We have previously uncovered a postsynaptic Dystrophin-dependent pathway whose malfunction results in changes in presynaptic function at the *Drosophila* neuromuscular junction. Here, we show that Dystrobrevin, a member of the Dystrophin Glycoprotein complex, is delocalized from the postsynaptic region in the absence of Dystrophin leading to an increased level of neurotransmitter release. Targeted relocalization of Dystrobrevin to the postsynaptic region in the Dystrophin mutant background restores neurotransmitter release to wild type levels. Dystrobrevin delocalization causes a reduction in the activity of the Rho-GAP Crossveinless-c leading to increased activity of the Rho-GTPase CDC42. Postsynaptic expression of constitutively-active CDC42 in the wild type background results in increased neurotransmitter release indicating that it is an important target of this pathway. We further show the colocalization of CDC42 and Dystrobrevin in the subsynaptic reticulum which supports our findings that these genes interact. Finally we present evidence that postsynaptic $Ca^{2+}$/calmodulin-dependent kinase II, which was previously implicated in retrograde signaling at this synapse, is a likely downstream target of CDC42. Taken together, our results outline a postsynaptic Dystrophin Glycoprotein Complex (DGC)-dependent pathway, comprised of highly evolutionarily-conserved proteins, which regulates presynaptic function. Disruption of this pathway results in an overly high homeostatic endpoint of neurotransmitter release. Similar defects at Dystrophin-deficient brain synapses may underlie the cognitive defects presented by a significant subset of Duchenne Muscular Dystrophy patients.

## Introduction

Neurons induce the depolarization of their targets, other neurons and muscles, by releasing neurotransmitters into the synaptic cleft where they bind to the opposing postsynaptic receptors. Release is tightly regulated, both during development and in the adult, to ensure that appropriate levels of neurotransmitter are delivered to the target.

The need for dynamic regulation of neurotransmitter release during development is well-exemplified by the neuromuscular junction (NMJ), the site of the innervation of a muscle fiber by a motoneuron. In *Drosophila*, for example, the embryonic muscle grows some 100-fold during the three stages of larval development. To match the increasing requirements for more neurotransmitter, the motoneuron presynaptic terminal expands and can therefore deliver more glutamate upon being evoked by upstream neurons. Thus, a simple increase in the size of the synapse allows the delivery of more neurotransmitter.

Neurotransmitter release levels in the non-growing adult must also be regulated to balance intersecting neural circuits such as those in the brain. So-call homeostatic plasticity mechanisms make local or global adjustments to compensate for alterations in neuronal excitability or synaptic strength that can otherwise destabilize the circuit or individual synapses [1]. These alterations may be the result of age, neuronal trauma, disease, or other dysfunction and include changes in membrane excitability, in neurotransmitter release machinery, or in postsynaptic receptor functions.

Both pre- and postsynaptic mechanisms underlying homeostatic plasticity have been uncovered. Presynaptic modifications include increases in the number of vesicle release sites, elevated probabilities of vesicle release and increased quantal size which reflects the amount of neurotransmitter in a single synaptic vesicle. Postsynaptic modifications include alterations in the size of the postsynaptic density and changes in the numbers of neurotransmitter receptors.

Local homeostatic plasticity requires communication from the target back to the innervating neuron. Such signaling pathways have been inferred in both mammalian and *Drosophila* studies focused on understanding synapse dynamics (reviewed in [2–5] ). They have been uncovered from the observation of changes in presynaptic function following the perturbation of postsynaptic responsiveness to neurotransmitter release. This was first illustrated by the finding that myasthenia gravis patient NMJs, whose acetylcholine receptors (AChR) are inhibited by autoantibodies, display upregulation of neurotransmitter release [6], [7]. Similar observations were made in mouse models where AChR function was compromised [8], [9] and at *Drosophila* neuromuscular junctions with diminished postsynaptic glutamate receptor function ([10–12]) or with impaired depolarization due to expression of an outwardly-directed K+ channel [13]. Furthermore, QC increases at the NMJ is when $Ca^2$+/Calmodulin-dependent Kinase II (CaMKII) activity is reduced postsynaptically by expression of an CaMKII-derived inhibitory peptide [14], [15]. In each of these cases, postsynaptic alterations elicit changes in presynaptic function, thus indicating the likely existence of a retrograde signaling pathway from the muscle to the motoneuron. Despite considerable efforts, little is known about the diffusible molecules or trans-synaptic protein complexes likely mediating retrograde signaling.

We have previously identified roles of Dystrophin protein isoforms at two different *Drosophila* synapses [16], [17]. Dystrophin is the gene whose mutation underlies Duchenne Muscular Dystrophy [18]. The absence of the large actin-binding Dystrophin isoform in humans results in progressive muscle degeneration with frequently-associated cognitive disabilities [19], [20]. The best-studied roles of the Dystrophin protein are those at the sarcolemma, where as a part of the large Dystrophin Glycoprotein Complex (DGC), it forms a stabilizing link between the actin cytoskeleton and the extracellular matrix [21]. The DGC consists of Dystrophin, Dystrobrevin

(DYB), Dystroglycan, the Syntrophins, the Sarcoglycans and, in mammals, Sarcospan. Significant numbers of studies over the past decade have revealed that, in addition to its role in protecting the muscle membrane against exercise-induced degeneration, the DGC acts to scaffold a number of signaling molecules to localize their functions (reviewed in [22]). Finally, while Dystrophin and it closely related ortholog, Utrophin, have long been known to be present at several types of mammalian synapses (reviewed in [20], [23]), much of their functions there remains to be determined.

The postsynaptic DLP2 Dystrophin isoform is required to maintain wild type levels of motoneuron neurotransmitter release at the *Drosophila* NMJ. Its absence from the subsynaptic reticulum (SSR) results in high QC, increased numbers of T-bars (presynaptic release sites) and an elevated probability of release [16]. The absence of Dystrophin also results in reduced activity or levels of the Rho-GAP, CV-C [24]. Rho-GAPs enhance the conversion of active GTP-bound Rho-GTPases to their inactive GDP-bound forms. The decrease in CV-C activity, in turn, results in an increase in the activity of the Rho-GTPase CDC42 [24] which effects the postsynaptic modifications changes resulting in increased neurotransmitter release from the motoneuron. We have also shown that the Dystrophin Dp186 isoform is required in the postsynaptic motoneuron to maintain normal levels of release from its innervating interneuron at a defined cholinergic interneuronal synapse in the *Drosophila* CNS [17]. Dp186 is apparently localized to motoneuron dendrites which are immediately postsynaptic to the interneuron. Thus, distinct Dystrophin isoforms play similar roles at two different types of synapses.

DYB, or Dystrophin-related protein, was identified as a Dystrophin-interacting protein at the Torpedo electric organ postsynaptic membrane [25–27] and has also been demonstrated to be present at the sarcolemma and neuromuscular junction in various species [28], [29]. In this study, we report that it is the delocalization of DYB from the SSR that likely underlies the Dystrophin DLP2 mutant NMJ phenotype. We further demonstrate that CDC42, which is enriched in the SSR and colocalizes with Dystrophin and DYB, is likely the chief postsynaptic target of this pathway. The postsynaptic expression of constitutively-active CDC42 alone is sufficient to elevate neurotransmitter release. Finally, we find that CDC42 likely acts to modulate the activity of CaMKII which itself was previously implicated in the maintenance of normal neurotransmitter release at the NMJ. This work describes, to our knowledge, the first multi-member postsynaptic pathway which controls presynaptic function.

## Materials and Methods

### Fly stocks

$w^{1118}$, the genetic background in which the *Dyb* mutation was generated, was used as the wild type control genotype for all experiments. The *Dys* DLP2 isoform null mutant allele, $Dys^{E6}$, was described previously [16]. The Df(3R)Exel6184 deficiency ("Df Dys") uncovers the entire Dystrophin locus. Df(2R)Exel6061 and Df(2R)aichi$^4$ are overlapping deficiencies which uncover the *Dyb* gene (FlyBase). $cdc42^4$ [30] and $cv\text{-}c^1$ [24], [31] are loss of function and hypomorphic alleles, respectively. The following GAL4 driver lines were used: 24B-GAL4 [32], mhc-GAL4 [10], [33], elav-GAL4 [34], and OK6-GAL4 [35]. A transgenic RNAi line targeting the cdc42 mRNA (transformant ID 100794) was obtained from the Vienna *Drosophila* RNAi Center. UAS-*CaMKII-T287A*, UAS-*CaMK–T287D* and UAS-*Ala* were described previously [36] and encode calcium-independent, constitutively-active and inhibitory forms of CaMKII, respectively. UAS-$cdc42^{V12}$ [34] is a constitutively-active transgenic allele of cdc42. UAS-*GFP*-$cdc42^{WT}$ was previously described [37]. Heatshock-regulated FLP and FLP/ISce1 lines [38] were used in the generation of the *Dyb*. UAS-Dystrobrevin-PA-encoding sequences were PCR amplified from wild type embryonic first-strand cDNA, cloned into the Gateway pENTR vector (Invitrogen), recombined into the pTWM (gift from Terence Murphey; www.ciwemb.edu/labs/murphy/ Gateway%20 vectors .html) vector and introduced into wild type flies to allow expression of MYC-tagged Dystrobrevin protein under control of tissue-specific GAL4 drivers [32]. The 11 amino acid sequence from Shaker which targets heterologous proteins to the subsynaptic reticulum [39] was appended to the carboxyterminus of UAS-*Dyb* A/B by insertion of an oligonucleotide into the pTWM-*Dyb* A/B construct described above. All P-element constructs were verified by sequencing. Crosses and generation of recombinant chromosomes were performed by standard *Drosophila* genetic approaches.

### Generation of the Dystrobrevin mutant

The *Dyb* gene was targeted by homologous recombination Ends-out targeting [40–42]. The region encoding the carboxyterminal domain common to all DYB isoforms was replaced by the *white* gene (**Fig. 2**). The targeting construct was generated as follows: *Dyb* homology region A and C were amplified from wild type genomic DNA using the primers *Dyb* region A forward, CGTACGCATCATCTGCATTGCTGTCA, *Dyb* region A reverse, GGCGCGCCTAA-GTTCTCAAGACCTAAGT; *Dyb* region C forward, GGTACCGGAGCAGCTCAACAA-GATTA and *Dyb* region C reverse, GCGGCCGCTAGAGCATTTAGAATTTGAT and TA-cloned into the pGEMT vector (Promega). Homology regions A and C were generated by digests with *Bsi*W1/*Asc*1 and *Acc*651/*Not*1 and ligated into the *Bsi*W1-*Asc*1 and *Acc*651-*Not*1 sites of the pW25 vector, respectively. The construct was transformed into the germ line of wild type flies at BestGene, Inc. Two inserts on the 3rd chromosome were identified and determined to be mobilizable upon provision of Flippase. Crosses for targeting were carried out at 25° C. The crossing scheme is shown (**Sup. Fig.1A**). Red-eyed final progeny were analyzed by PCR using the following primers: F1, TATTGTGCCAGGCATAGGTG: R1, GTGTTTCTCAAGAGC- TGCGC; F2, GCGTAAACC- GCTT GGAGCTTC; R2, CTGGCTCTATGCCGTTACGAT. Other primer sequences are available upon request. Southern blotting was performed to further verify the targeting. DNA was prepared from flies homozygous for the putative targeted allele, digested with EcoR1 and Hind3, separated by agarose gel electrophoresis, and then transferred to nylon membranes. The membranes were probed with a dioxygenin-labeled homology region A and C DNA fragments and hybridizing fragments were detected using a chemiluminiscent assay (Roche).

**Generation of anti-Dystrobrevin antisera and other immuno-reagents used**

Rabbit antisera were raised against two GST-tagged Dystrobrevin antigens: 1) anti-DYBCO$_2$H (encoded by base pairs 1842-2408 of the Dystrobrevin A transcript, Genbank accession number NM_165904) and 2) anti-DYBmid (encoded by base pairs 1294-1818). Other primary antibodies used were anti-actin (MP Biomedicals), anti-HRP (Promega), anti-*Dys*CO2H [16], anti-DLG (DSHB; [43], [44]), anti-DGluRIIA (DSHB; [45]) , anti-DGlurRIIB (gift from A. DiAntonio; [46]), anti-dS3 (gift from M. Kelley; [47]), anti-CDC42 (gift from U. Tepass; [48]) anti-GFP (Molecular probes, Invitrogen) and the anti-Fas2 1D4 [33] and anti-Bruchpilot nc82 (gift from A. Hofbauer; [49], [50]) monoclonal antibodies (DSHB). AlexaFluor-conjugated secondary antibodies (Invitrogen) and HRP-conjugated secondary antibodies (Jackson Immunoresearch Laboratories) were used as described [16]. Standard epifluorescence or confocal microscopy was used to visualize and photograph the samples.

**Quantification of bouton number and muscle size**

Body walls of third instar larvae were stained with an FITC-conjugated anti-HRP (Jackson Immunoresearch Laboratories). Photographs of body wall muscle number 4 in segments A2-A5 for each genotype were made from at least 5-10 larvae (40-80 muscles in total) and muscle areas were measured using ImageJ (NIH). The numbers of boutons in these same preparations were counted.

**Immunohistochemistry**

Third instar larvae were dissected in ice-cold PBS and body walls were fixed in 4% formaldehyde in PBS and then incubated overnight at 4° C with the anti-Bruchpilot NC82 monoclonal antibody [50] followed by application of goat anti-mouse Alexa Fluor 488 antibody. Body wall synapses were visualized by confocal microscopy (Leica TCS SL, Leica Microsystems) and the number of nc82-positive domains at synapses on muscles 6 and 7 in 5 segments (A2-A6) were counted and total bouton area measured and analyzed using the Leica Application Suite software.

**Transmission electron microscopy**

Larval dissection, fixation, embedding, and sectioning were performed as described [16]. Semi-serial sections of body walls from $w^{1118}$ and the dystrobrevin mutant were prepared and electron micrographs were made of Type Ib boutons on muscles 6 and 7 using a transmission electron microscope (Tecnai 12 Biotwin, FEI, Eindhoven, The Netherlands).

**Electrophysiology**

To minimize possible genetic background effects, we backcrossed each mutant allele or transgenic chromosome against wild type control flies for at least 5 generations prior to using them in electrophysiological analyses. Electrophysiological recordings were performed as describe [16]. Briefly, a microelectrode filled with 3 M KCl was inserted into muscle 6 (segments A3–A4) of dissected third-instar female larvae bathed in HL3 containing 0.6 mM $Ca^{2+}$ unless described otherwise [51]. The intracellular measurements were recorded using a Geneclamp 500B amplifier (Axon Instruments, Union City, CA), low-pass filtered at 10 kHz, high-pass filtered at 0.5 Hz, and digitized using a Digidata 1322A and pClamp9 software (Axon Instruments). mEJPs were recorded continuously for 1 min. 30 EJPs were recorded at 0.3 Hz stimulation after the appropriate axon was stimulated by a pulse generator (Master-8, AMPI, Jerusalem, Israel) via a suction electrode. Electrical input resistance of all muscle fibers recorded was above 4 mΩ. The mean mEJP amplitude and frequency were analyzed by using the peak detection feature of Mini-analysis 6.0 (Synaptosoft, Decatur, GA); all events were confirmed by eye. EJP amplitudes were analyzed using Clampfit 9.0 and amplitudes were normalized to a

membrane potential of -60 mV. NMJ quantal content (QC) was calculated by dividing the mean EJP amplitude (calculated from 30 events) corrected for non-linear summation (B.A. Stewart, personal communication) by the mean mEJP amplitude (calculated from 100 events). Paired-pulse facilitation was assessed at 0.6 mM, 0.4 mM and 0.2 mM $Ca^{2+}$ using 50 ms interstimulus intervals. All primary electrophysiological data are presented in the Supplemental Table.

### Statistical analyses

The program GraphPad Prism version 5 was used for statistical analysis. One way ANOVA was performed with least significant differences (LSD) or Bonferroni for post hoc multiple comparisons for statistical analyses. Differences were considered significant when $p<0.05$; *, ** and *** indicate $p<0.05$, $p<0.01$ and $p<0.001$, respectively.

## RESULTS

### Localization of DYB at the neuromuscular junction and generation of a *Dyb* mutant.

There are seven DYB protein isoforms encoded by the single *Drosophila Dyb* gene (http://flybase.org/cgi-bin/gbrowse/dmel/?Search=1;name=FBgn0033739). Their individual expression patterns have not been reported, however RNA in situ analyses using a probe common to all isoforms indicates that they are expressed in the muscle and nervous system [52]. We generated two different antisera recognizing epitopes in DYB common to all isoforms. Specifically, one immunogen, anti-DYBCO2H, contained a carboxyterminal region while the other, anti-DYBMid, contained sequences encoding the middle portion of the protein (details in Materials and Methods). Staining of 3rd larval instar body walls with anti-$DYBCO_2H$ reveals that DYB is present throughout the muscle and is particularly enriched at synaptic boutons (**Fig. 1B**). Anti-DYBMid gave a similar staining pattern (data not shown). DYB is present both pre- and postsynaptically at the bouton as evidenced by high magnification visualization of boutons co-labeled with anti-$DYBCO_2H$ and the presynaptic marker anti-horseradish peroxidase [53] (**Fig. 1C** inset). We focus on the postsynaptic functions of DYB in this report.

We generated a mutant allele of *Dyb*, $Dyb^{11}$, by performing "ends-out" homologous recombination [40], [41]. We validated the molecular structure of the knockout by PCR and Southern blotting (**Fig. 1D** and **Sup. Fig. 1**). Five of the seven isoforms' ATG translational initiator codon and the region encoding the domains responsible for DYB's protein-protein interactions, the EF Hand [54] and ZZ domains [55], were replaced by the *white* eye color gene. Thus, the $Dyb^{11}$ is almost certainly a null allele of *Dyb*. Homozygous mutants are viable and do not display obvious visible phenotypes. Staining of the wild type 3rd larval central nervous system with anti-$DYBCO_2H$ reveals that DYB is expressed in the neuropile, the thoracic neuromeres and several higher order structures in the brain lobes, including the optical system (**Fig. 1E**). This pattern is similar to that previously observed for the CNS-specific Dystrophin isoform, DP186 [17]. In contrast, the *Dyb* mutant 3rd larval instar CNS does not detectably express DYB (**Fig. 1F**).

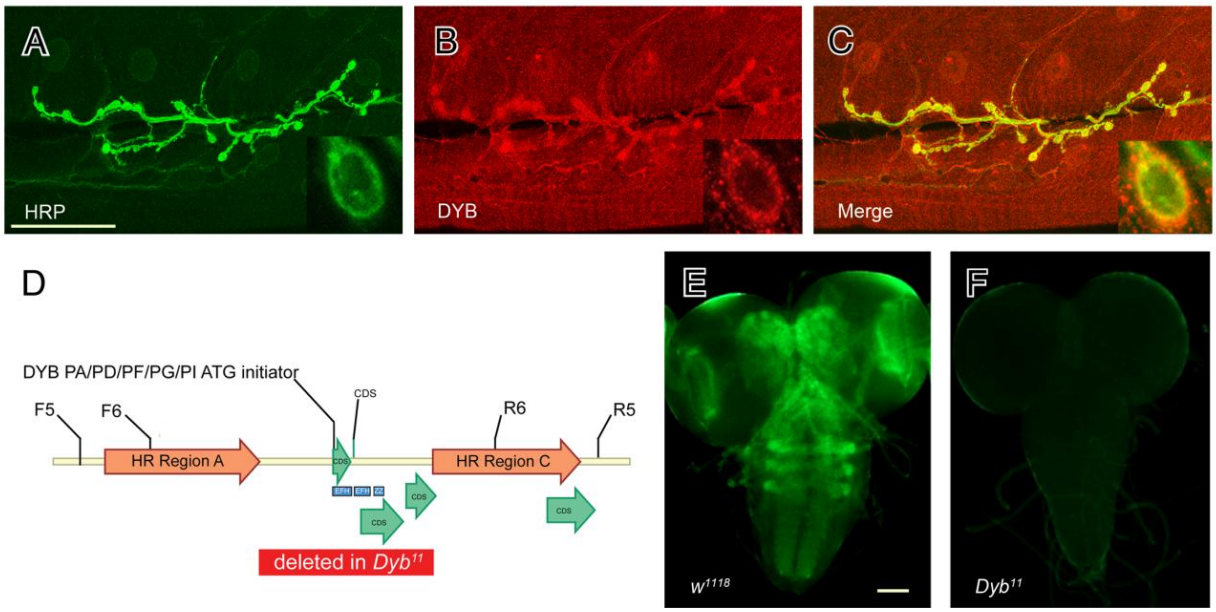


**Figure 1. DYB is localized at the NMJ and the mutant lacks DYB expression.** Wild type 3rd larval instar body walls were stained with anti-HRP (**A**), recognizing a presynaptic marker [53] and anti-DYBCO$_2$H (**B**) with the merged images shown in (**C**). High magnification images of a single bouton are shown in the insets at the lower right hand side of each panel. DYB is present in the muscle, with particular enrichment in the SSR and it also colocalizes with the anti-HRP signal. The *Dyb* genomic region is shown in (**D**). The regions used for the donor homologous recombination construct (HR Regions A and C), the initiator codon employed by five of the seven DYB isoforms, CDS-encoding exons, the regions encoding the EF-Hand and ZZ domains common to all DYB isoforms and the locations of the primer hybridizing sites use to confirm targeting events are shown. The region of the *Dyb* gene replaced by the *white* eye color gene is indicated. Anti-DYBCO$_2$H staining of wild type (**E**) and *Dyb*$^{11}$ mutant (**F**) 3rd larval instar brain/neuropiles are shown. DYB protein is not detectable in the mutant. Scale bar = 50 µm

## *Dyb* mutants display increased numbers of boutons due to the absence of postsynaptic protein.

The overall NMJ structure in the *Dyb* mutant is similar to that of the wild type control (**Fig. 2B**). Furthermore, stainings with antibodies recognizing several proteins located at the synapse, the glutamate receptors, DGluRIIA [45] and DGluRIIB [12], the Fasciclin protein, Fas2 [33], and the SSR-associated scaffolding protein, Discs-large (DLG; [44], [56]), indicate apparently wild type levels and localization of these proteins in the mutant background (**Sup. Fig. 2**). Quantitation of bouton numbers visualized by anti-HRP staining at two different synapses, however, indicates an approximately 25% increase in the number of boutons per synapse in the *Dyb* mutant (**Fig. 2C**). Staining of the *Dyb* mutant synapse with the mAb nc82, which recognizes Bruchpilot, a component of the presynaptic vesicle-docking T-bar structure [50], indicates that there are wild type numbers of active zones per bouton (**Fig. 2D-F;** quantitation in **2G**). We previously demonstrated that the numbers of nc82 positive punctae correlate with the number of T bars visualized by electron microscopy [24]. Thus, there does not seem to be an increase in the vesicle docking machinery in the *Dyb* mutant.

Synapse side-specific rescue experiments indicate that postsynaptic, but not presynaptic, expression of DYB in the *Dyb* mutant background restores bouton counts to wild type levels (**Fig. 2H**). In conclusion, the absence of DYB from the muscle therefore results in increased numbers of boutons while the number of active zone per bouton remains unaffected.

**Bouton ultrastructure is altered in the *Dyb* mutant.**

We employed electron microscopy on serial sections of *Dyb* mutant body walls to examine potential changes in synaptic ultrastructure (**Fig. 3A and B**). Quantification of SSR per bouton area reveals that the *Dyb* mutant displays slight increases in the size of the SSR, a zone of highly folded membrane in the muscle closely associated with the motoneuron terminus (**Fig. 3C**). Furthermore, we observe a dramatic increase in so-called "patched areas" within the SSR (indicated in **Fig. 3B** by arrows; quantified in **3D**). As these areas resemble arrays of ribosomes, we stained body walls with an anti-ribosomal protein dS3 antibody [47], [57], and find that there is an increase in bouton staining in the *Dyb* mutant (**Fig. 3I**), indicating that the patched areas are indeed likely ribosomes.

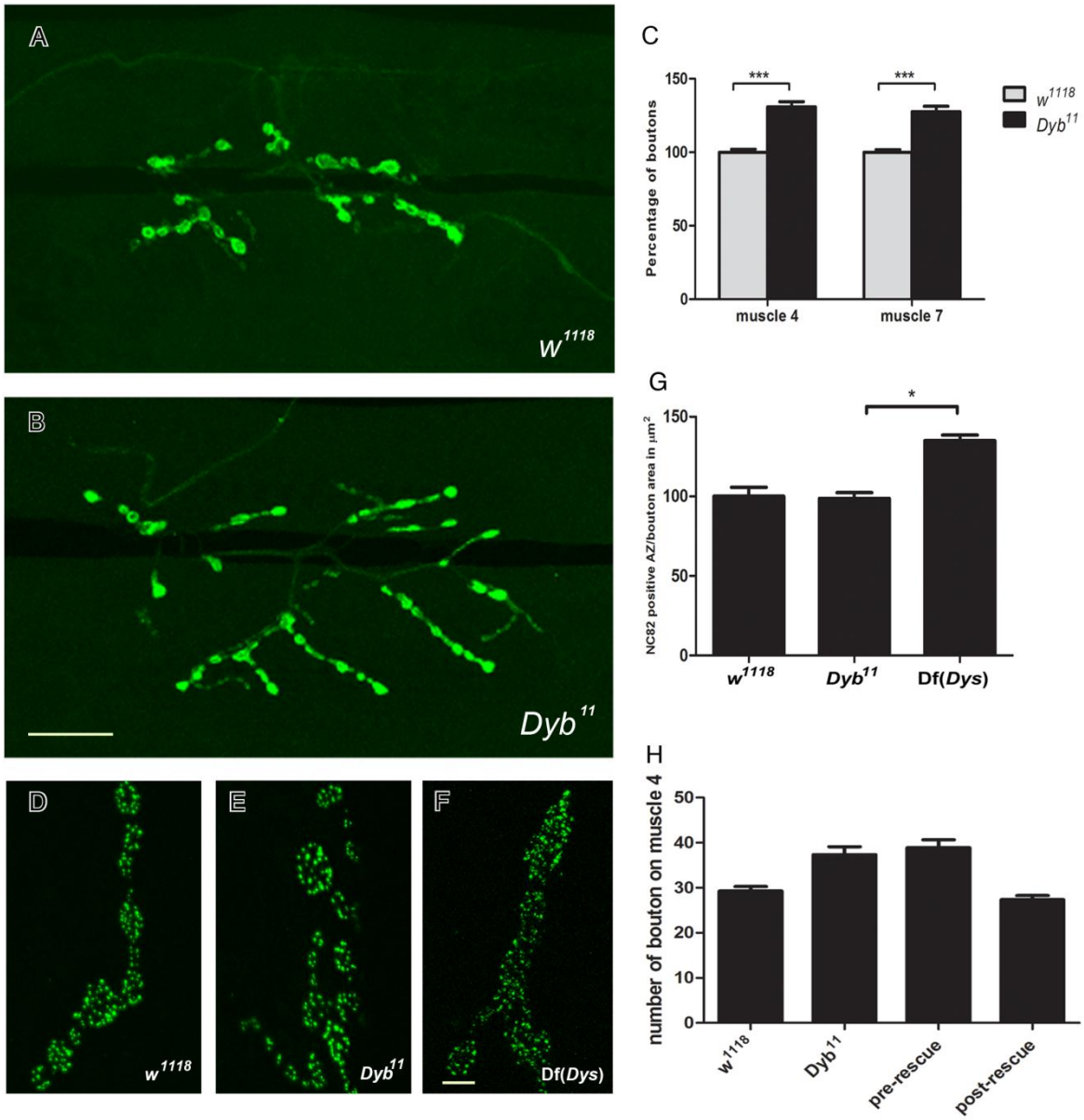


**Figure 2. The Dyb mutant displays increased numbers of synaptic boutons, wild type numbers of nc82$^{+}$ active zones and the bouton phenotype is rescued by postsynaptic expression of DYB.** Wild type ($w^{1118}$) (**A**) and $Dyb^{11}$ mutant (**B**) synapses at muscle 6/7 visualized with anti-HRP are shown. Quantitation of boutons at the muscle 4 and muscle 6/7 synapses reveals an ~ 25% increase in bouton count (**C**). Anti-Bruchpilot (mAb nc82) stainings of wild type (**D**), $Dyb^{11}$ mutant (**E**) and Dystrophin deficiency (Df(Dys), **F**) are shown. The $Dyb^{11}$ mutant displays wild type numbers of nc82$^{+}$ active zones while, as previously reported for the $Dys^{DLP2\ E6}$ mutant , animals

homozygous for the Dystrophin deficiency have increased numbers of nc82$^{+}$ active zones (quantitation in **G**). Quantitation of pre- vs. postsynaptic rescue is shown (**H**). Expression of UAS-DYB driven by the postsynaptic 24B-GAL4 driver (post-rescue), but not by the OK6-GAL4 presynaptic driver (pre-rescue), rescues the *Dyb*$^{11}$ mutant increased bouton phenotype. Scale bar of A and B = 25 µm. Scale bar of D, E and F = 5 µm.

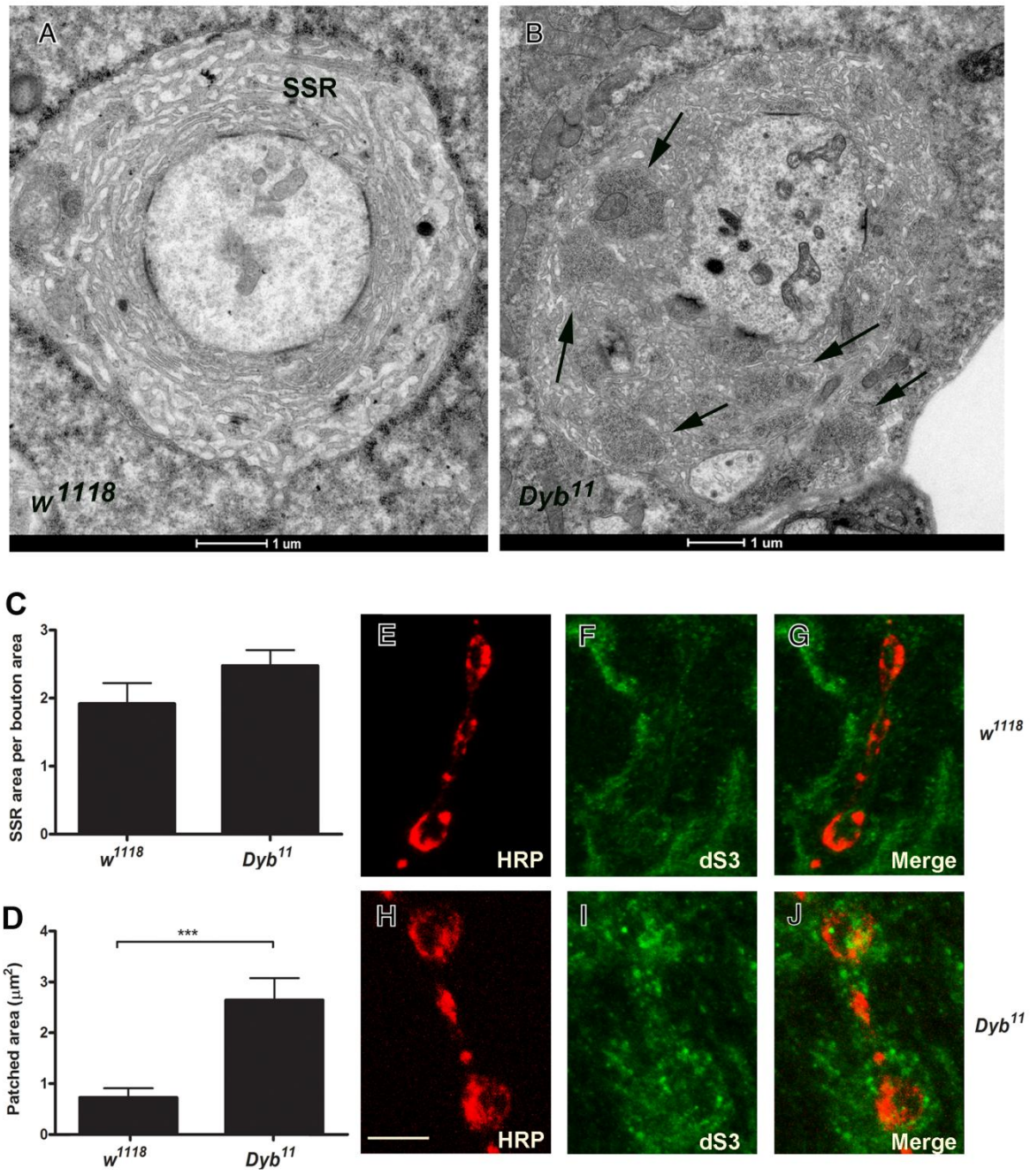


**Figure 3. The *Dyb* mutant exhibits ultrastructural alterations at the synaptic bouton.** Electron micrographs of single wild type (**A**) and *Dyb*$^{11}$ mutant (**B**) boutons are shown. The *Dyb*$^{11}$ mutant has slightly increased SSR area normalized to total bouton area relative to the wild type control (quantitation in **C**) and includes patched areas, likely ribosomes (indicated by arrows in **B**; quantitation in **D**). mouse anti-Synapsin mAb (**E** and **H**), rabbit anti-ribosomal protein dS3 (**F** and **I**) and merged images (**G** and **J**) are shown for wild type (**E**-**G**) and *Dyb*$^{11}$ mutant synapses (**H**-**J**). The mutant synapse exhibits increased bouton-associated staining for the ribosomal protein supporting the likelihood that the patched areas in the electron micrographs of the *Dyb*$^{11}$ mutant synapses are arrays of ribosomes. Scale bar = 5 µm.

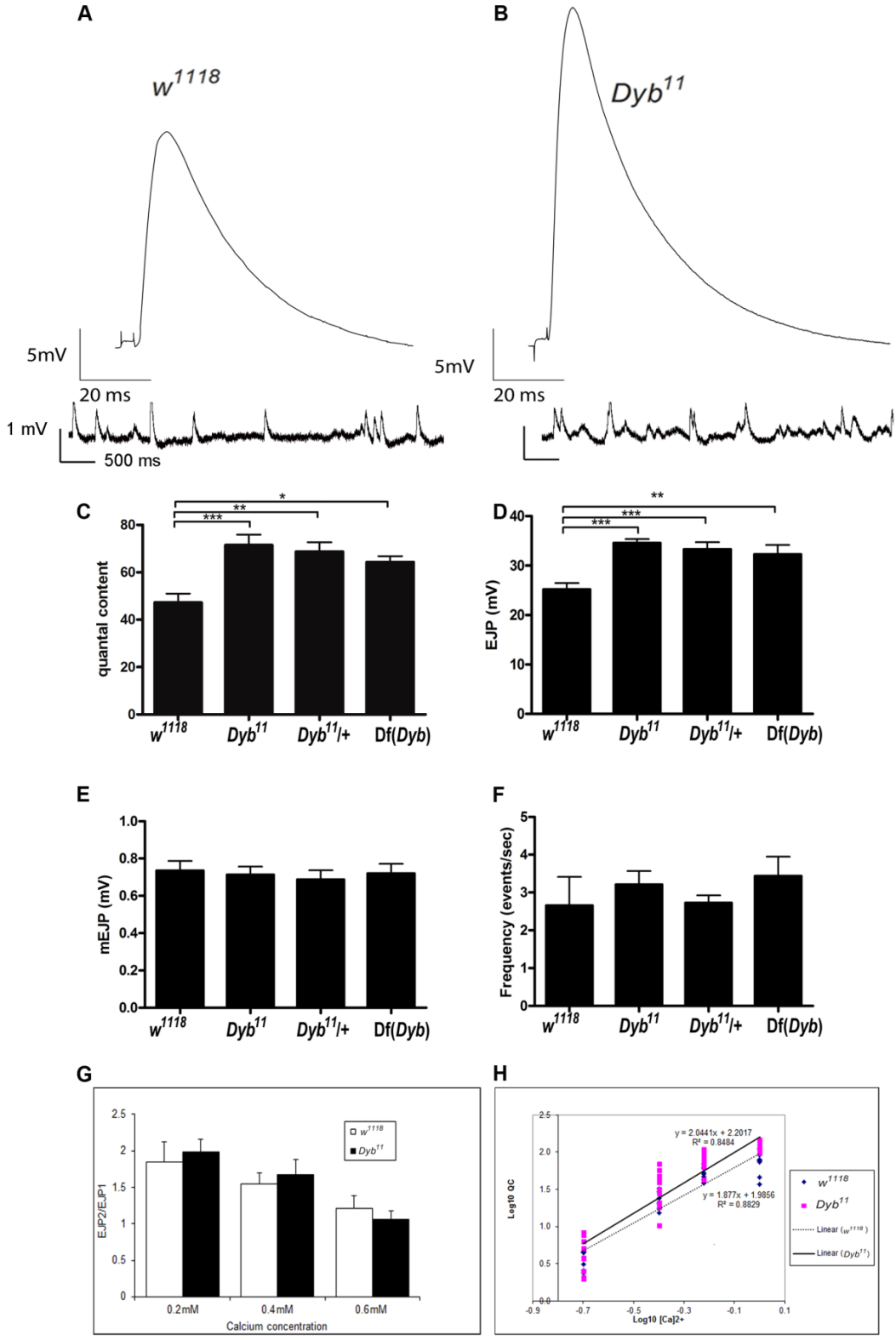


**Figure 4. *Dyb* mutants display increased neurotransmitter release.** Traces of EJP and mEJP recordings at wild type (**A**) and $Dyb^{11}$ mutant (**B**) synapses are shown. $Dyb^{11}$ has significantly increased EJP amplitudes. QC (**C**), EJP amplitudes (**D**), and mEJP amplitude (**E**) and frequency (**F**) are shown for wild type, homozygous vs. heterozygous $Dyb^{11}$ mutants and a transheterozygous combination of deficiencies [Df(*Dyb*) or (Df(2R)Exel6061/Dr(2R)achi$^4$) ] both of which uncover the *Dyb* genomic locus. All mutant combinations exhibit increased QC. Pulse-paired facilitation analyses were performed at four $Ca^{2+}$ concentrations. The $Dyb^{11}$ mutant, similarly to the wild type, does not display facilitation (**G**), nor does it display altered response to changes in external $Ca^{2+}$ concentration (**H**).

***Dyb* mutant exhibits increased quantal content at the NMJ.**

We evaluated the physiology of the *Dyb* mutant synapse by performing intracellular microelectrode electrophysiological recordings. The $Dyb^{11}$ mutant displays a significant increase in the amplitude of the evoked responses (EJPs) with no apparent differences in the miniature evoked junctional potential amplitudes (mEJPs) (compare **Fig. 4A** and **B**). This leads to increased quantal content (QC) relative to controls (**Fig. 4C**). QC reflects the level of neurotransmitter release and is calculated by dividing the mean EJP amplitude by the mean mEJP amplitude. Transheterozygotes bearing independently-derived overlapping deficiencies uncovering the *Dyb* locus show similarly increased QC (**Fig. 4C**). Animals heterozygous for $Dyb^{11}$ also display increased QC indicating that, like the Dystrophin (DLP2 isoform; [16], and *cv-c* genes [24], *Dyb* is haploinsufficient for its function at the NMJ.

We determined whether an increase in the probability of vesicle release underlies the increased QC at the $cv\text{-}c^{1}$ mutant NMJ by performing paired-pulse facilitation (PPF). PPF is a form of short-term adaptation of synaptic transmission [58] and is quantified by calculation of the ratio of the amplitudes of two consecutive EJPs evoked at short interstimuli intervals. When the probability of release of EJP1 decreases, as is observed at lower external $Ca^{2+}$concentrations, PPF increases [59], [60]. The *Dyb* mutant was found to display wild type PPF at three $Ca^{2+}$ concentrations indicating that it does not have an increase in the probability of vesicle release (**Fig. 4G**). Comparison of the mutant QCs with those of controls at four external $Ca^{2+}$ concentrations ranging from 0.2 to 1.0 mM revealed no change in $Ca^{2+}$ -cooperativity of neurotransmitter release in the mutant (**Fig. 4H**). Therefore, the properties of the $Ca^{2+}$ sensors that regulate $Ca^{2+}$-dependent vesicle fusion are likely not altered in the *Dyb* mutant.

To evaluate whether DYB is required either pre- or postsynaptically to maintain wild type neurotransmitter release, we performed synapse-side specific rescue experiments in the *Dyb* mutant background. We find that, similarly to the increased bouton count phenotype, it is the absence of postsynaptic DYB which causes the observed increased neurotransmitter release (**Fig. 5**).

**DYB is delocalized from the Dystrophin-deficient synapse and its relocalization to the SSR restores *Dystrophin* mutant QC to wild type levels.**

DYB is no longer localized to the synaptic bouton in animals lacking all Dystrophin isoforms (**Fig. 6B**), indicating that a DGC-like complex, which disappears in the absence of Dystrophin, exists at the NMJ. Western blot analyses of mutant body wall extract proteins reveal that they contain wild type levels of DYB (**Fig. 6I**), indicating that delocalization of DYB, rather than its degradation, is the reason for its absence from the *Dystrophin* mutant synapse.

We hypothesized that the increase in QC in the *Dystrophin* mutant background might be due to the delocalization of DYB. To address this, we generated fly lines expressing DYB tagged with an eleven amino acid sequence derived from the Shaker protein previously shown to target heterologous proteins to the SSR [39]. Targeting by this sequence is due to its interaction with Discs-large protein (DLG) [61] which is found both pre- and postsynaptically at the NMJ [44]. The tagged protein localizes to the boutons in the absence of Dystrophin when expressed under control of a muscle-specific (**Fig. 6C**) or a motoneuron-specific GAL4 driver (**Fig. 6D**). Wild type DYB is also delocalized from the sarcomere in the *Dystrophin* mutant background, however the SSR-targeted species did not relocalize to the sarcomere in the absence of Dystrophin (data not shown). Expression of the tagged protein postsynaptically, but not presynaptically, restores QC to wild type levels in the *Dystrophin* mutant background (**Fig. 6F**) further demonstrating that the postsynaptic delocalization of DYB likely underlies the

*Dystrophin* mutant QC phenotype. Rescue of the *Dystrophin* mutant QC phenotype by expression of tagged DYB, which localizes to the SSR, but not the sarcomere, indicates that it is DYB in the SSR, and not at the sarcomere, which regulates the homeostatic QC endpoint.

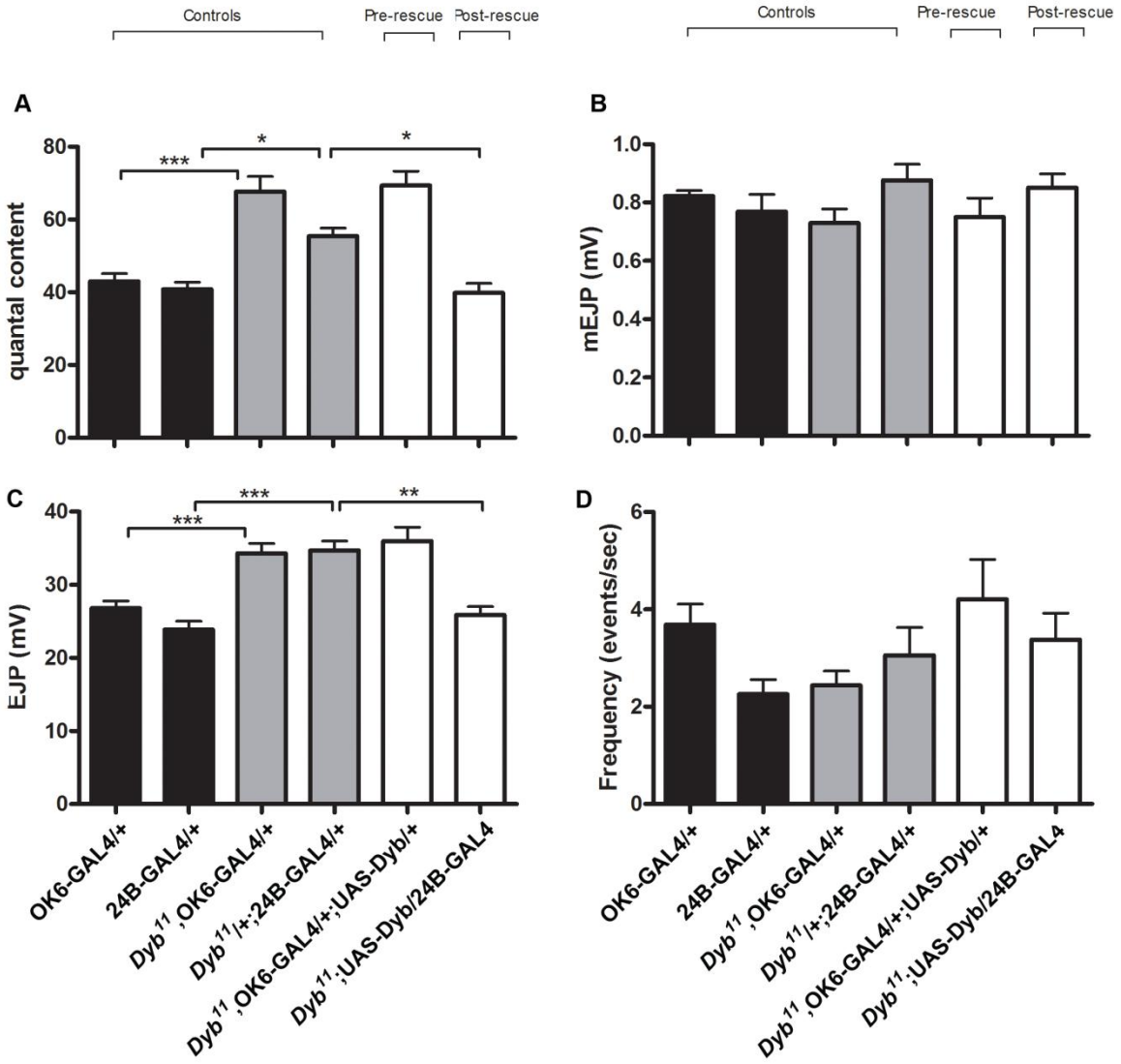


**Figure 5. The *Dyb*$^{11}$ mutant increased QC phenotype is rescued by postsynaptic DYB expression.** To evaluate which side of the synapse DYB needs be expressed to maintain wild type levels of neurotransmitter release, we evaluated the physiology of synapses where DYB was expressed either pre- or postsynaptically in the *Dyb*$^{11}$ mutant background. The QC (**A**), amplitude of EJPs (**B**) and mEJP amplitudes (**C**) and frequencies (**D**) for the genotypes indicated in the figure are shown. Expression of DYB driven by the postsynaptic 24B-GAL4 driver, but not that driven by the presynaptic OK6-GAL4 driver, rescues the high *Dyb*$^{11}$ mutant QC to wild type levels.

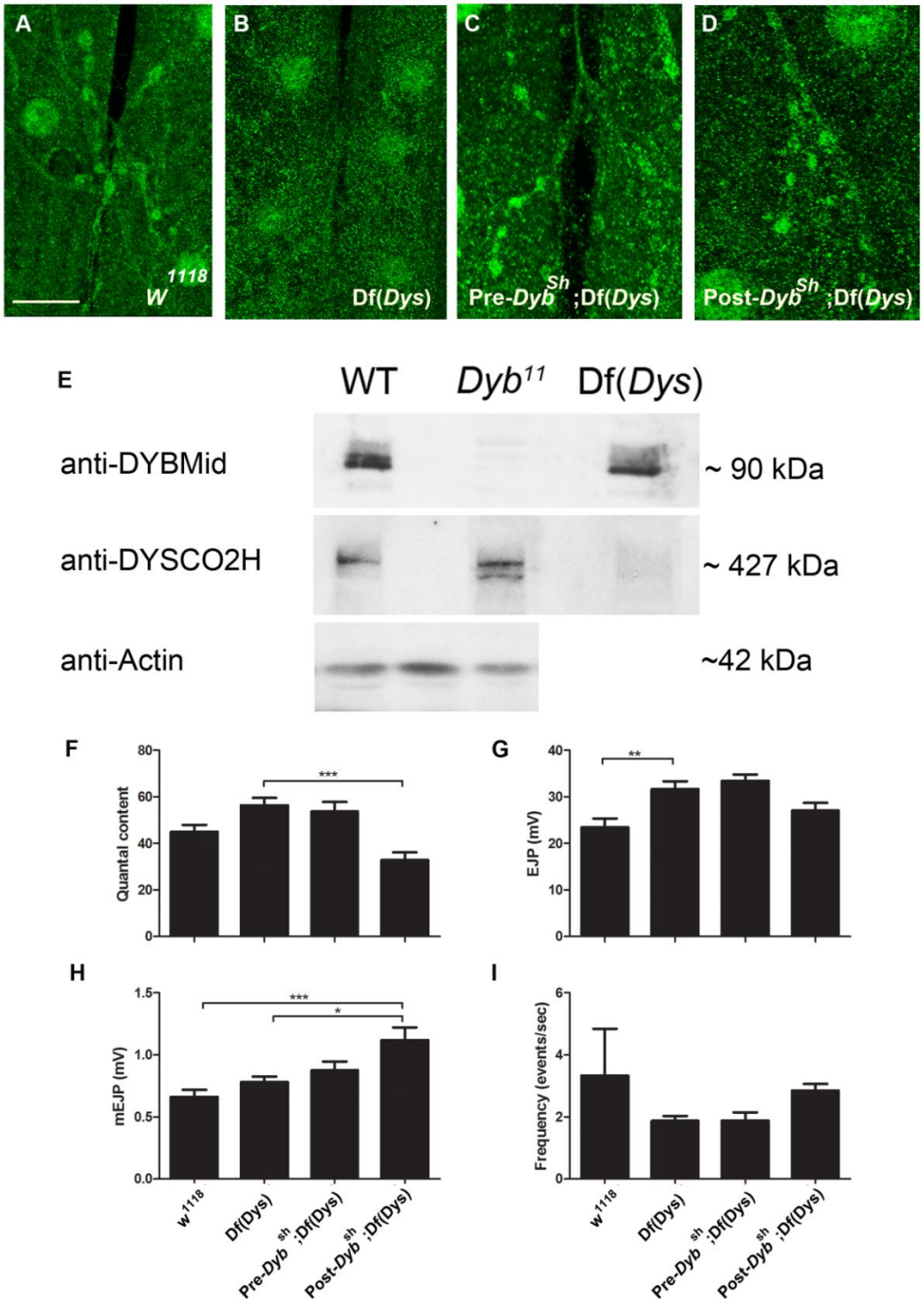


**Figure 6. DYB is delocalized from the Dystrophin-deficient synapse and relocalization of DYB to the postsynaptic region of the bouton (post-*Dyb*$^{sh}$;Df(Dys)) rescues the *Dystrophin* mutant high QC phenotype.** Anti-DYBCO$_2$H-stained wild type (**A**), homozygous Df(Dys) (**B**) and the *Dyb*$^{11}$ mutant presynaptically (**C**) or postynaptically (**D**) expressing the synapse-targeted DYB species are shown. DYB is no longer detectable at the boutons in the *Dystrophin* mutant indicating that it is likely delocalized. Expression of the synapse-targeted DYB in both the postsynaptic and presynaptic compartment restores DYB to the synapse in the *Dystrophin* mutant background. Immunoblots of wild type, *Dyb*$^{11}$ mutant and Dystrophin deficiency 3$^{rd}$ larval instar body wall lysates detected with anti-DYBMid and anti-Dystrophin are shown (**E**). DYB is present at wild type levels in the Dystrophin-deficient animals indicating that its absence from the boutons is due to delocalization and not degradation. Data from electrophysiological recordings of the synapse-targeted and controls are shown; QC (**F**), EJP amplitudes (**G**), mEJP amplitudes (**H**) and frequencies (**I**). Postsynaptic, but not presynaptic, expression of synapse-targeted DYB suppresses the high QC observed in the *Dystrophin* mutant background. Scale bar = 25 µm.

**DYB acts through the Rho-GTPase CDC42 and CaMKII to regulate neuro-transmitter release.**

We and others had previously found that the *Dystrophin* gene plays roles during wing vein patterning [24], [62], [63]. Homozygous *Dystrophin* mutants display alterations in the formation of the posterior cross vein (PCV); it is either absent or fails to connect to one or both adjacent longitudinal veins. These studies employed the heterozygous *Dystrophin* mutant as a sensitized background in which to uncover *Dystrophin*-interacting genes in transheterozygous tests. We therefore evaluated whether mutant alleles of Dystrophin and *Dyb* interact. Homozygous *Dyb* mutant wings have wild type PCVs (**Sup. Fig. 3A**) as do heterozygous *Dystrophin* mutant wings (**Sup. Fig. 3D**). Simultaneous homozygosity for *Dyb* and heterozygosity for *Dystrophin*, however, reveals that these genes interact during formation of the PCV (**Sup. Fig. 3F**; quantitation in **3G**). Experiments performed with $Dyb^{11}$ and the $cv\text{-}c^{1}$ allele resulted in a similar pattern of interaction (**Sup. Fig. 4**). Thus, *Dyb* functionally interacts with both *Dystrophin* and *cv-c* during wing vein formation.

We have previously shown that the increase in QC in the *Dystrophin* mutant could be prevented by heterozygosity for a null allele of *cdc42* or by postsynaptic expression of dsRNA targeting the *cdc42* transcript [24], indicating that CDC42 activity is increased in the *Dystrophin* mutant background. We find that expression of *cdc42*-specific dsRNA or heterozygosity for a null mutant allele of *cdc42* also prevents the increase in QC in the *Dyb* mutant background (**Fig. 7A**). Further support for the existence of an interaction between DYB and CDC42 comes from our observation that they colocalize in the SSR (**Fig. 7G**). CDC42 appears to be actively concentrated in the SSR as evidenced by the high level of accumulation of GFP-CDC42 there when it is overexpressed in the muscle (**Fig 7H**). The interactions between CDC42 or CV-C and DYB are unlikely, however, to be direct; neither protein co-immunoprecipitates with DYB under conditions where DYB can be co-immunoprecipitated with the Dystrophin Dp186 protein (data not shown).

Previous reports indicate that decreased postsynaptic functionality of the $Ca^{2+}$/calmodulin-dependent kinase, CaMKII, caused by expression of an inhibitory fragment of the protein, Ala, result in increased QC at the NMJ [14], [15]. The appearance of boutons with reduced CaMKII activity is very similar to those in the *Dyb* mutant; the SSR is larger and contains an increased numbers of ribosomes [64]. We therefore determined whether CaMKII interacts with the Dystrophin/DYB/CDC42 pathway.

Postsynaptic expression of a $Ca^{2+}$-independent constitutively-active CaMKII protein (CaMKII-T287D) suppresses QC to wild type levels in the *Dyb* mutant background (**Fig. 8A**). Expression of CaMKII-T287A, which cannot become $Ca^{2+}$-independent, does not reduce the high *Dyb* mutant QC. Since increased CaMKII activity suppresses the *Dyb* mutant phenotype, we therefore conclude that the Dyb-dependent pathway normally acts to activate CaMKII in the wild type background. Since we observe no obvious changes in CaMKII levels or localization in the Dystrophin or *Dyb* mutant backgrounds (data not shown), the absence of Dystrophin or DYB likely leads to reduction in the CaMKII activity. This in turn leads to elevated neurotransmitter release. Thus, increasing the amount of active CaMKII in the *Dyb* mutant background prevents the increase in QC.

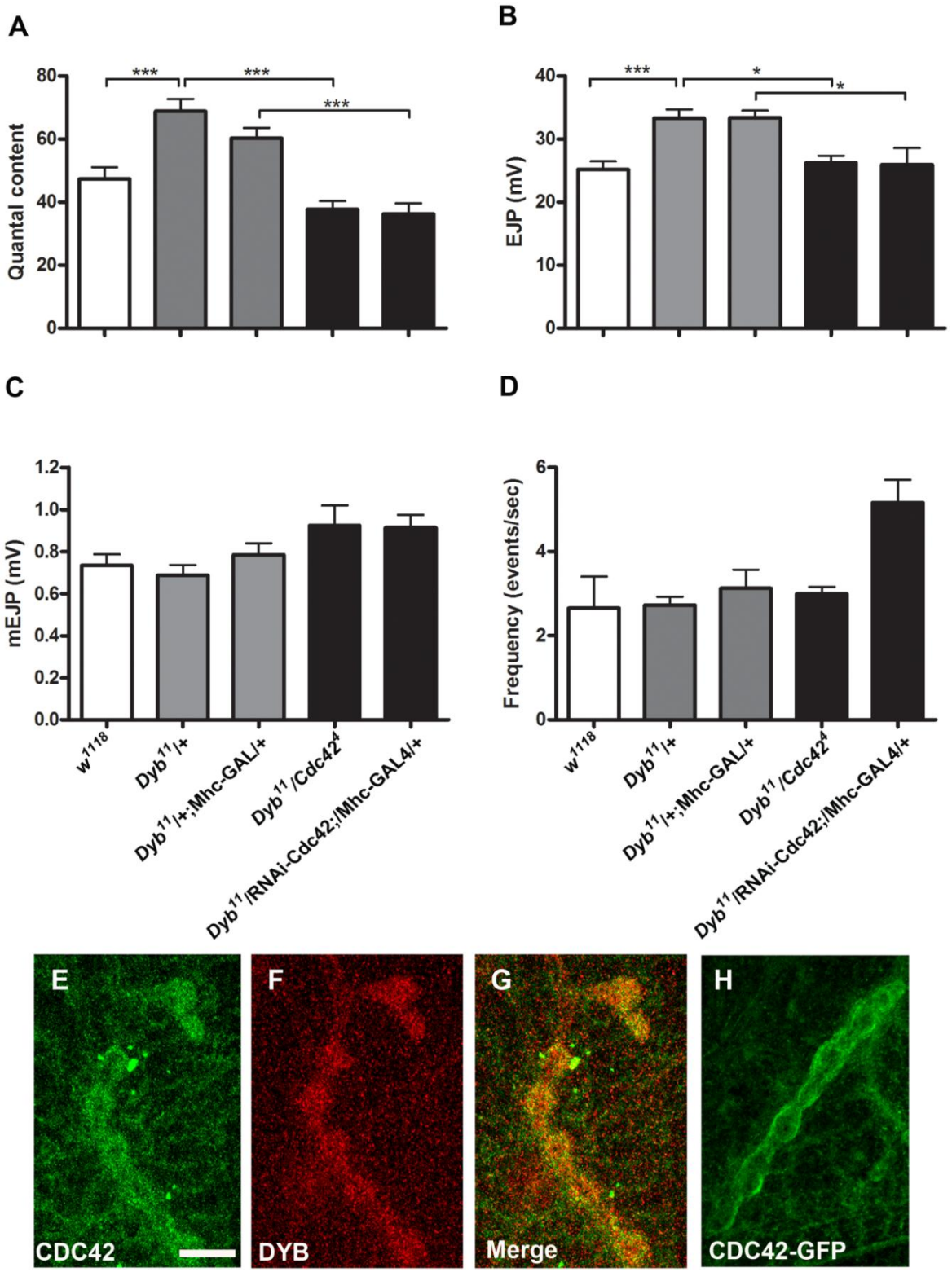


**Figure 7. Reduction in CDC42 expression levels rescue the *Dyb* mutant increased QC phenotype and CDC42 colocalizes with DYB in the SSR.** Electrophysiological recordings of the genotypes indicated in the figure were performed. QC (**A**), EJP amplitudes (**B**), mEJP amplitudes (**C**) and frequencies (**D**) are shown. Reduction of CDC42 expression by removing one copy of the wild type gene ($cdc42^4$/+) or by postsynaptic expression of a *cdc42*-targeting dsRNA (RNAi-Cdc42) suppresses the high *Dyb* mutant QC. Wild type 3rd larval instar body walls were stained with anti-CDC42 (**E**), anti-DYB$CO_2$H (**F**) with the merge shown in (**G**). CDC42 and DYB colocalize in the SSR. The accumulation of overexpressed GFP-CDC42 in the SSR is shown (**H**). These results indicate that CDC42 activity is increased in the *Dyb* mutant background and that CDC42 and DYB can physically interact. Scale bar = 10 µm.

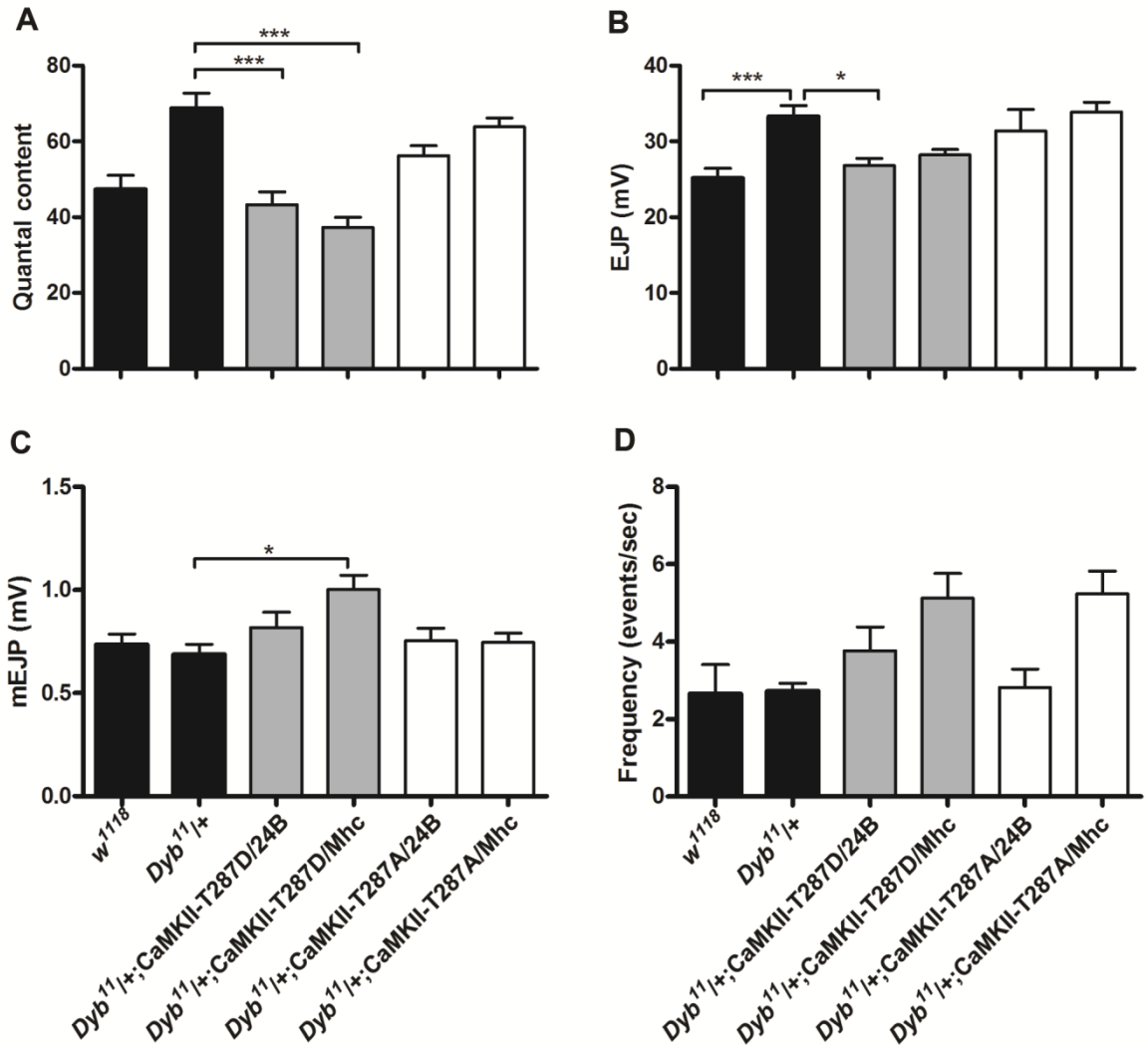


**Figure 8. Increased CaMKII activity suppresses the high QC in the *Dyb* mutant background.** Electrophysiological recordings of the genotypes indicated in the figure were performed. QC (**A**), EJP amplitudes (**B**), mEJP amplitudes (**C**) and frequencies (**D**) are shown. Expression of the constitutively-active CaMKII T287D protein, but not the T287A protein, driven by either of two muscle-specific drivers (24B-GAL4 or Mhc-GAL4) suppresses the high *Dyb* mutant QC.

We find that postsynaptic expression of a constitutively-active CDC42-encoding transgene (UAS-*CDC42*$^{V12}$) alone results in QC levels equivalent to those observed in *Dystrophin* and *Dyb* mutants (**Fig. 9**). This result indicates that CDC42 is likely a primary target of the postsynaptic Dystrophin/DYB/CV-C pathway regulating presynaptic neurotransmitter release. Simultaneous expression of constitutively-active CaMKII and CDC42 transgenes results in wild type QC levels (**Fig. 9**) providing further support for our hypothesis that CaMKII is a positively-regulated target of the wild type pathway.

To further evaluate whether CaMKII is likely a target of the pathway, we performed an epistatic test. As mentioned above, postsynaptic expression of the CaMKII inhibitory peptide, Ala, was previously shown to result in increased QC [14], [15]. We have demonstrated that heterozygosity for a null allele of *cdc42* suppresses both the *Dystrophin* [16] and *Dyb* mutant (this work) increased QC phenotypes. If CDC42 is downstream of CaMKII, we expect that reduction of its levels would suppress the increased QC observed when Ala is expressed in the muscle. This was not the case (**Fig. 10**) indicating that CaMKII is likely downstream of CDC42.

At present, however, we cannot rule out the possibility that CaMKII is part of another postsynaptic pathway, parallel to that containing Dystrophin, DYB and CDC42, which also regulates presynaptic neurotransmitter release.

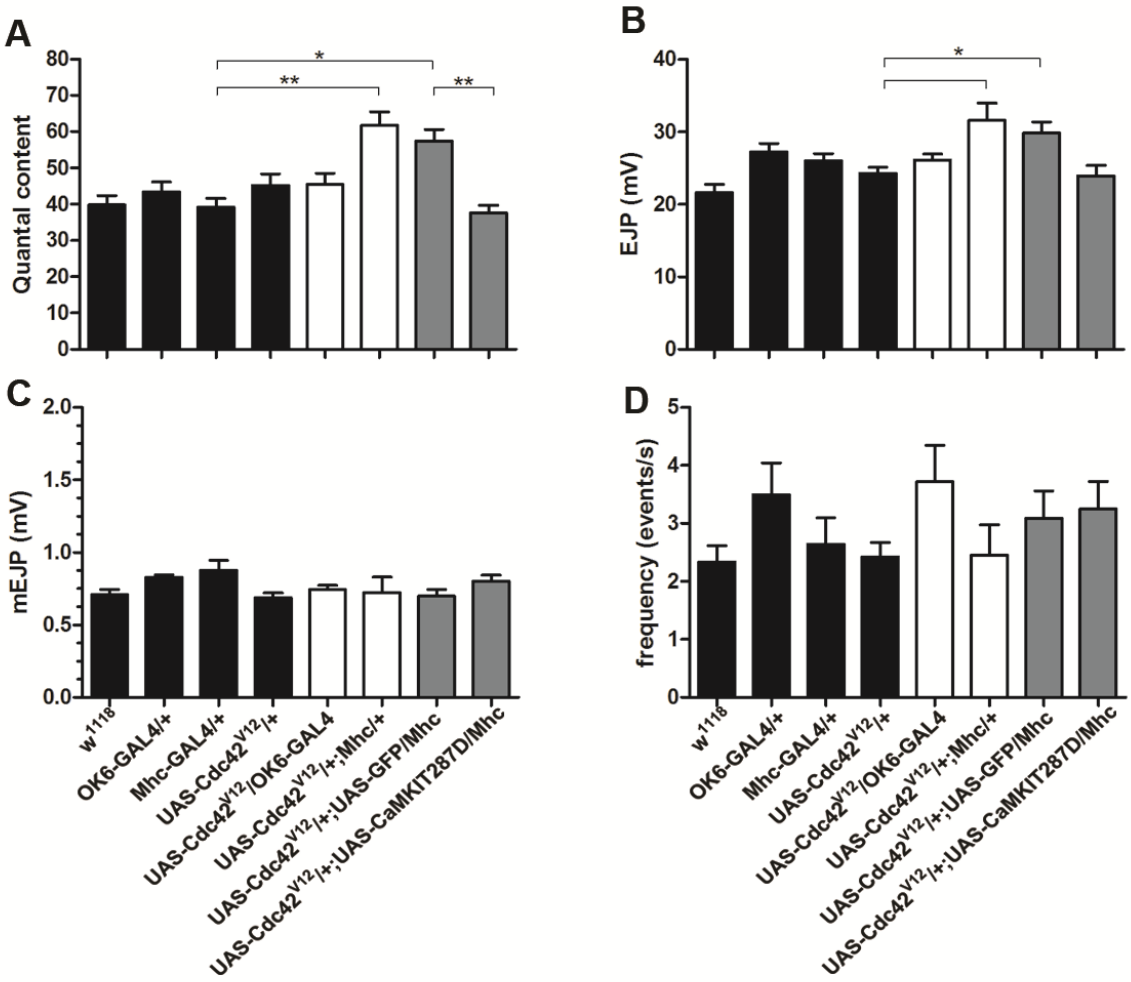


**Figure 9. Expression of constitutively-active CDC42 alone is sufficient to increase QC and this increase is suppressed by elevation of CaMKII activity.** Electrophysiological recordings of the genotypes indicated in the figure were performed. QC (**A**), EJP amplitudes (**B**), mEJP amplitudes (**C**) and frequencies (**D**) are shown. QC significantly increases upon postsynaptic overexpression of the constitutively-active $CDC42^{V12}$ protein and this increase is blocked by simultaneously expressing constitutively-active CaMKII protein.

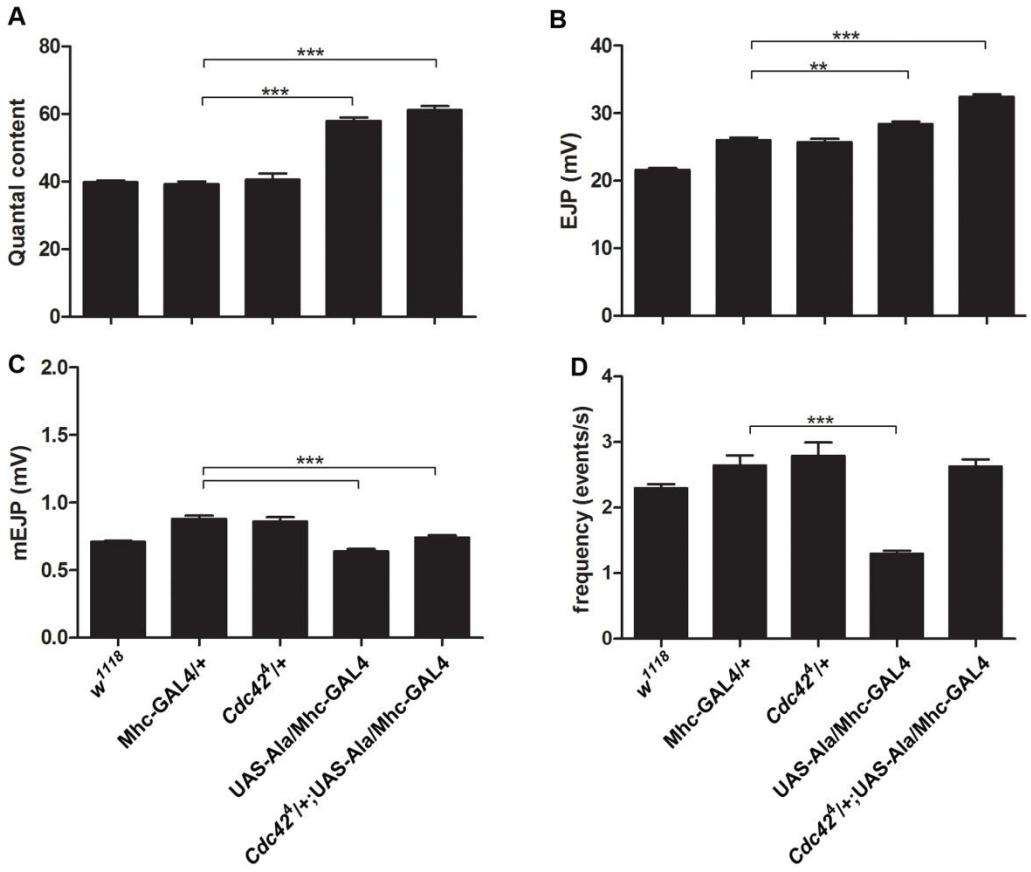


**Figure 10. Reduction in CDC42 expression levels does not suppress the high QC observed upon postsynaptic inhibition of CaMKII.** Electrophysiological recordings of the genotypes indicated in the figure were performed. QC (**A**), EJP amplitudes (**B**), mEJP amplitudes (**C**) and frequencies (**D**) are shown. QC was significantly increased upon postsynaptic overexpression of the CaMKII inhibitory peptide, Ala, as previously reported [14], [15]. Heterozygosity for *cdc42* does not block this increase.

## Discussion

In this study we describe a postsynaptic signaling pathway, scaffolded by the DGC in the SSR, which regulates the homeostatic endpoint of neurotransmitter release at the *Drosophila* NMJ. To our knowledge, although a number of signaling pathway members are known to be associated with the DGC (review in [22]), this is the first description of a DGC-dependent signaling pathway whose functional target is known. The absence of the postsynaptic DGC results in increased CDC42 activity which possibly acts to suppress postsynaptic CaMKII activity leading to increased neurotransmitter release by the motoneuron. A schematic model of this pathway is presented (**Sup. Fig. 5**).

We determined that DYB is present at both the pre- and postsynaptic compartments at the NMJ. Furthermore, we demonstrated that DYB is delocalized from the NMJ in the absence of all Dystrophin. We previously reported that the Dystrophin DLP2 isoform is localized in the postsynaptic region [16]. Taken together, these results indicate that DLP2 and DYB form a DGC-like complex in the SSR at the NMJ.

DYB is also expressed in the embryonic and larval nervous systems in patterns remarkably similar to that of the central nervous system-specific Dystrophin Dp186 isoform [17], e.g., in the presumptive embryonic motoneuron dendrites and throughout the larval neuropile and thoracic neuromeres, respectively. In unpublished experiments, we have found that DYB remains

appropriately localized in the larval CNS in the *Dys* $^{Dp186}$ mutant (data not shown), indicating that DYB is localized there in a Dystrophin-independent fashion or that other Dystrophin isoforms in addition to Dp186 are expressed in motoneurons. Our observation that DYB is delocalized from the larval neuropile in animals homozygous for a chromosomal deficiency uncovering the entire Dystrophin locus supports the latter possibility. The expression patterns of all of the identified *Drosophila* Dystrophin isoforms have been determined [17], [52], [65] and, except Dp186, they are not apparently expressed in the neuropile. Thus, there are likely other *Drosophila* Dystrophin isoforms remaining to be uncovered.

Our finding that the *Dyb* mutant NMJ exhibits elevated QC and that DYB is delocalized in the *Dystrophin* mutant background raised the question as to whether it is the absence of DYB from the synapse that underlies the *Dystrophin* mutant increased neurotransmitter release phenotype. Our results indicate that this is likely the case. Restoration of DYB to the SSR, but not the presynaptic compartment, in the *Dystrophin* mutant background by fusion of the wild type DYB protein to a short targeting tag derived from the SHAKER protein [39] suppressed the *Dystrophin* mutant high QC phenotype. Thus, it is apparently the postsynaptic delocalization of DYB from the SSR that causes the *Dystrophin* mutant increased QC phenotype.

While the *Dyb* mutant, like the *Dys*$^{DLP2\ E6}$ [16] and Df(Dys) (this study) mutants, displays increased QC at the NMJ and SSR-targeted DYB rescues the Df(Dys) mutant QC phenotype, there are significant differences between the *Dyb*, *Dys*$^{DLP2\ E6}$ and Df(Dys) mutant phenotypes. In the case of the *Dys*$^{DLP2\ E6}$ [16] and Df(Dys) (data not shown) mutants, there is decreased PPF indicating an increased probability of release while decreased PPF was not observed in the *Dyb* mutant. The DYB–deficient and Df(Dys) (data not shown) NMJs, but not those of the *Dys*$^{DLP2\ E6}$ [16] mutant display increased numbers of synaptic boutons. Finally, while the numbers of T-bars are significantly higher in both *Dystrophin* mutants than in controls (this study and [16]) they are not increased in the *Dyb* mutant. The Df(Dys) mutant NMJ likely, therefore, displays a compound phenotype, specifically, elevated QC and increased numbers of boutons due to the delocalization of DYB from the SSR and increased numbers of presynaptic release sites resulting from DYB-independent mechanisms. This hypothesis is supported by our observation that postsynaptic expression of the SSR-targeted DYB species rescues the increased bouton count phenotype in the Df(Dys) mutant background but does not suppress the increased number of T-bars (data not shown).

The increase in presynaptic nc82$^{+}$ foci in either of the two *Dystrophin* mutant backgrounds is unlikely be due to the delocalization of DYB since no such increases were observed at the *Dyb* mutant NMJ. Thus, postsynaptic Dystrophin likely acts to scaffold at least two signaling pathways regulating presynaptic function, one DYB-dependent and the other not. Furthermore, taken together with the observed increase in QC at the DYB-deficient NMJ without an increase in release sites, these data indicate that the increase in release sites in the *Dystrophin* mutants is unlikely to account for the increased levels of neurotransmitter release.

Further supporting the hypothesis that DYB and Dystrophin act together is our observation that the two genes show similar interactions with *cv-c* during wing vein formation and with *cdc42* in the regulation of QC at the NMJ. In particular, both the *Dys*$^{DLP2\ E6}$ [24] and *Dyb*$^{11}$ (this work) mutant high QC phenotypes are suppressed by heterozygosity for a null mutant allele of *cdc42* or by postsynaptic expression of *cdc42*-targeting dsRNA both of which result in a reduction of CDC42 activity.

We found that postsynaptic expression of constitutively-active CDC42 in an otherwise wild type background is sufficient to result in increased presynaptic neurotransmitter release to levels similar to those observed in the *Dystrophin* [16], *cv-c* [24] and *Dyb* (this work) mutant backgrounds. Taken together with our previous observations that the other *Drosophila* Rho-

GTPases are unlikely to be involved in this pathway [24], this result indicates that CDC42 is a primary postsynaptic target of this pathway. We also demonstrate that CDC42 colocalizes with DYB in the SSR indicating that it is possible for the proteins to interact.

Finally, we show that the increased QC, observed in both the *Dyb* mutant background and when constitutively-active CDC42 is expressed postsynaptically, is suppressed by simultaneous postsynaptic expression of constitutively-active CaMKII. This is particularly interesting since CaMKII was previously implicated in a retrograde signaling mechanism which sets an appropriate homeostatically-controlled neurotransmitter release endpoint at the NMJ [14], [15]. Our genetic epistasis tests indicate that *cdc42* is unlikely to be downstream of *CaMKII*. Thus, if these proteins are in the same pathway, it is likely that CAMKII is downstream of CDC42.

What is the relationship between our findings and those in other species, specifically with respect to the roles of DYB at the synapse? To the best of our knowledge, only limited electrophysiological studies have been performed in any of the other Dystrobrevin-deficient models, specifically those in mouse and *C. elegans*, making close comparison with our current findings difficult. Morphological and behavioral alterations exhibited by Dystrobrevin-deficient animals, however, indicate that Dystrobrevins play roles at both peripheral and central synapses.

Mammals have two Dystrobrevin genes, Dystrobrevin-α (DTNA) and Dystrobrevin-β (DTNB) each encoding several distinct protein isoforms (reviewed in [29], [66], [67]). DTNB is expressed primarily in non-muscle tissues, e.g., the brain, lung liver and kidneys. DTNA is considered to be muscle-specific; however its expression during development is quite dynamic and includes domains within the nervous system and other tissues [68]. Studies of mice lacking DTNA [69–71], revealed that they display irregular distributions of acetylcholine receptors, reductions in the number of junctional folds and loss of neuronal nitric oxide synthase (nNOS) at the NMJ. Only a relatively subtle central nervous system phenotype, a slight reduction in the size and numbers of $GABA_A\alpha1$ receptors in cerebellar Purkinje cells, was exhibited by DTNB knockout mice [72]. Mice lacking both DTNA and DTNB, however, have a significant reduction in $GABA_A\alpha1$ foci and performed poorly, relative to controls, in balance and sensorimotor tests [72] suggesting that the Dystrobrevins play an important role in cerebellar synaptic functions.

*C. elegans* has a single Dystrobrevin ortholog-encoding gene, *dyb-1* which is expressed in most, if not all, muscle and neurons but not detectably in other tissues [73], [74]. *dyb-1* mutant animals display similar behavioral phenotypes to those lacking Dystrophin, specifically, hyperactivity and hypercontraction during locomotion [73], [74]. They are also sensitive to increases in acetylcholine which correlates with the observation that *dyb-1* mutant muscles depolarize at lower concentrations of acetylcholine than controls [74]. Strikingly, with respect to our findings, overexpression of *dyb-1* was shown to rescue the behavioral phenotypes of the *dystrophin* mutant [75]. Thus, Dystrobrevin and Dystrophin also interact at the synapse in the nematode.

The clear genetic interactions of *cdc42* with *Dystrophin* and *Dyb* in the regulation of neurotransmitter release, the colocalization of CDC42 and DYB in the SSR and the ability of constitutively-active CDC42 to phenocopy the *Dystrophin* and *Dyb* mutant QC phenotypes underscore the importance of future studies aimed at identifying CDC42's targets in the postsynaptic density. By furthering our studies of this pathway, we will better understand the likely conserved roles of the DGC at the NMJ and orthologous complexes at other synapses.

## Acknowledgments

We thank Mariska van der Plas and Anneke Kremer for generating the UAS-Dyb constructs and transformants and preliminary characterization of the anti-DYB antisera, Bert van Veen for assistance with the fly work and Monique Bansraj and Niels de Water for assistance with the molecular biology. We are grateful to A. Chiba, A. DiAntonio, A. Hofbauer, M. Kelley, U. Tepass, R. White, the Developmental Studies Hybridoma Bank, the Bloomington *Drosophila* Stock Center, and the *Drosophila* Genomics Resource Center for kindly providing fly lines, antibodies and plasmids. Finally, the comments of Jaap Plomp, Ron Habets and Isabel de Ridder improved the manuscript.

## Authors Contributions

The author(s) have made the following declarations about their contributions: Conceived and designed the experiments: SP GSKP LGF JNN. Performed the experiments: SP AWMdJ GSKP LGF JNN. Analyzed the data: SP GSKP LGF JNN. Wrote the paper: SP LGF JNN.

## References

[1] G. Turrigiano, “Too Many Cooks? Intrinsic and Synaptic Homeostatic Mechanisms in Cortical Circuit Refinement.,” *Annual review of neuroscience*, vol. 34, pp. 89-103, Jan. 2011.

[2] G. W. Davis, “Homeostatic control of neural activity: from phenomenology to molecular design.,” *Annual review of neuroscience*, vol. 29, pp. 307-23, Jan. 2006.

[3] G. W. Davis and I. Bezprozvanny, “Maintaining the stability of neural function: a homeostatic hypothesis.,” *Annual review of physiology*, vol. 63, pp. 847-69, Jan. 2001.

[4] K. Pozo and Y. Goda, “Unraveling mechanisms of homeostatic synaptic plasticity.,” *Neuron*, vol. 66, no. 3, pp. 337-51, May 2010.

[5] G. Turrigiano, “Homeostatic signaling: the positive side of negative feedback.,” *Current opinion in neurobiology*, vol. 17, no. 3, pp. 318-24, Jun. 2007.

[6] S. G. Cull-Candy, R. Miledi, and O. D. Uchitel, “Diffusion of acetylcholine in the synaptic cleft of normal and myasthenia gravis human endplates.,” *Nature*, vol. 286, no. 5772, pp. 500-2, Jul. 1980.

[7] J. J. Plomp, G. T. Van Kempen, M. B. De Baets, Y. M. Graus, J. B. Kuks, and P. C. Molenaar, “Acetylcholine release in myasthenia gravis: regulation at single end-plate level.,” *Annals of neurology*, vol. 37, no. 5, pp. 627-36, May 1995.

[8] J. J. Plomp, G. T. van Kempen, and P. C. Molenaar, “Adaptation of quantal content to decreased postsynaptic sensitivity at single endplates in alpha-bungarotoxin-treated rats.,” *The Journal of physiology*, vol. 458, pp. 487-99, Dec. 1992.

[9] A. W. Sandrock et al., “Maintenance of acetylcholine receptor number by neuregulins at the neuromuscular junction in vivo.,” *Science (New York, N.Y.)*, vol. 276, no. 5312, pp. 599-603, Apr. 1997.

[10] G. W. Davis and C. S. Goodman, “Genetic analysis of synaptic development and plasticity: homeostatic regulation of synaptic efficacy,” *Curr Opin Neurobiol*, vol. 8, no. 1, pp. 149-156, Feb. 1998.

[11] A. DiAntonio, S. A. Petersen, M. Heckmann, and C. S. Goodman, “Glutamate receptor expression regulates quantal size and quantal content at the Drosophila neuromuscular junction,” *J Neurosci*, vol. 19, no. 8, pp. 3023-3032, 1999.

[12] S. A. Petersen, R. D. Fetter, J. N. Noordermeer, C. S. Goodman, and A. DiAntonio, “Genetic analysis of glutamate receptors in Drosophila reveals a retrograde signal regulating presynaptic transmitter release,” *Neuron*, vol. 19, no. 6, pp. 1237-1248, Dec. 1997.

[13] S. Paradis, S. T. Sweeney, and G. W. Davis, “Homeostatic control of presynaptic release is triggered by postsynaptic membrane depolarization.,” *Neuron*, vol. 30, no. 3, pp. 737-49, Jun. 2001.

[14] A. P. Haghighi, B. D. McCabe, R. D. Fetter, J. E. Palmer, S. Hom, and C. S. Goodman, “Retrograde control of synaptic transmission by postsynaptic CaMKII at the Drosophila neuromuscular junction,” *Neuron*, vol. 39, no. 2, pp. 255-267, 2003.

[15] T. Morimoto, M. Nobechi, A. Komatsu, H. Miyakawa, and A. Nose, “Subunit-specific and homeostatic regulation of glutamate receptor localization by CaMKII in Drosophila neuromuscular junctions.,” *Neuroscience*, vol. 165, no. 4, pp. 1284-92, Feb. 2010.

[16] M. C. van der Plas, G. S. Pilgram, J. J. Plomp, A. de Jong, L. G. Fradkin, and J. N. Noordermeer, “Dystrophin is required for appropriate retrograde control of neurotransmitter release at the Drosophila neuromuscular junction,” *J Neurosci*, vol. 26, no. 1, pp. 333-344, 2006.

[17] L. G. Fradkin, R. A. Baines, M. C. van der Plas, and J. N. Noordermeer, “The dystrophin Dp186 isoform regulates neurotransmitter release at a central synapse in Drosophila,” *J Neurosci*, vol. 28, no. 19, pp. 5105-5114, 2008.

[18] E. P. Hoffman, R. H. Brown, and L. M. Kunkel, “Dystrophin: the protein product of the Duchenne muscular dystrophy locus.,” *Cell*, vol. 51, no. 6, pp. 919-28, Dec. 1987.

[19] C. Perronnet and C. Vaillend, “Dystrophins, utrophins, and associated scaffolding complexes: role in mammalian brain and implications for therapeutic strategies.,” *Journal of biomedicine & biotechnology*, vol. 2010, p. 849426, Jan. 2010.

[20] G. S. Pilgram, S. Potikanond, R. A. Baines, L. G. Fradkin, and J. N. Noordermeer, “The roles of the dystrophin-associated glycoprotein complex at the synapse,” *Mol Neurobiol*, vol. 41, no. 1, pp. 1-21.

[21] D. J. Blake, A. Weir, S. E. Newey, and K. E. Davies, “Function and genetics of dystrophin and dystrophin-related proteins in muscle.,” *Physiological reviews*, vol. 82, no. 2, pp. 291-329, Apr. 2002.

[22] T. A. Rando, “The dystrophin-glycoprotein complex, cellular signaling, and the regulation of cell survival in the muscular dystrophies,” *Muscle Nerve*, vol. 24, no. 12, pp. 1575-1594, 2001.

[23] A. Waite, C. L. Tinsley, M. Locke, and D. J. Blake, “The neurobiology of the dystrophin-associated glycoprotein complex,” *Annals of Medicine*, vol. 41, no. 5, pp. 344-359, 2009.

[24] G. S. K. Pilgram, S. Potikanond, M. C. van der Plas, L. G. Fradkin, and J. N. Noordermeer, “The RhoGAP crossveinless-c interacts with Dystrophin and is required for synaptic homeostasis at the Drosophila neuromuscular junction.,” *The Journal of neuroscience : the official journal of the Society for Neuroscience*, vol. 31, no. 2, pp. 492-500, Jan. 2011.

[25] M. H. Butler et al., “Association of the Mr 58,000 postsynaptic protein of electric tissue with Torpedo dystrophin and the Mr 87,000 postsynaptic protein.,” *The Journal of biological chemistry*, vol. 267, no. 9, pp. 6213-8, Mar. 1992.

[26] A. Cartaud et al., “Localization of dystrophin and dystrophin-related protein at the electromotor synapse and neuromuscular junction in Torpedo marmorata.,” *Neuroscience*, vol. 48, no. 4, pp. 995-1003, Jun. 1992.

[27] K. R. Wagner, J. B. Cohen, and R. L. Huganir, “The 87K postsynaptic membrane protein from Torpedo is a protein-tyrosine kinase substrate homologous to dystrophin,” *Neuron*, vol. 10, no. 3, pp. 511-522, Mar. 1993.

[28] H. M. Sadoulet-Puccio, T. S. Khurana, J. B. Cohen, and L. M. Kunkel, “Cloning and characterization of the human homologue of a dystrophin related phosphoprotein found at the Torpedo electric organ post-synaptic membrane.,” *Human molecular genetics*, vol. 5, no. 4, pp. 489-96, Apr. 1996.

[29] D. J. Blake, “Dystrobrevin dynamics in muscle-cell signalling: a possible target for therapeutic intervention in Duchenne muscular dystrophy?,” *Neuromuscular disorders : NMD*, vol. 12 Suppl 1, pp. S110-7, Oct. 2002.

[30] R. G. Fehon, T. Oren, D. R. LaJeunesse, T. E. Melby, and B. M. McCartney, “Isolation of mutations in the Drosophila homologues of the human Neurofibromatosis 2 and yeast CDC42 genes using a simple and efficient reverse-genetic method.,” *Genetics*, vol. 146, no. 1, pp. 245-52, May 1997.

[31] B. Denholm, S. Brown, R. P. Ray, M. Ruiz-Gómez, H. Skaer, and J. C.-G. Hombría, “crossveinless-c is a RhoGAP required for actin reorganisation during morphogenesis.,” *Development (Cambridge, England)*, vol. 132, no. 10, pp. 2389-400, May 2005.

[32] A. H. Brand and N. Perrimon, “Targeted gene expression as a means of altering cell fates and generating dominant phenotypes,” *Development*, vol. 118, no. 2, pp. 401-415, 1993.

[33] C. M. Schuster, G. W. Davis, R. D. Fetter, and C. S. Goodman, “Genetic dissection of structural and functional components of synaptic plasticity. II. Fasciclin II controls presynaptic structural plasticity,” *Neuron*, vol. 17, no. 4, pp. 655-667, 1996.

[34] L. Luo, Y. J. Liao, L. Y. Jan, and Y. N. Jan, “Distinct morphogenetic functions of similar small GTPases: Drosophila Drac1 is involved in axonal outgrowth and myoblast fusion.,” *Genes & development*, vol. 8, no. 15, pp. 1787-802, Aug. 1994.

[35] H. Aberle, A. P. Haghighi, R. D. Fetter, B. D. McCabe, T. R. Magalhaes, and C. S. Goodman, “wishful thinking encodes a BMP type II receptor that regulates synaptic growth in Drosophila,” *Neuron*, vol. 33, no. 4, pp. 545-558, 2002.

[36] P. Jin, L. C. Griffith, and R. K. Murphey, “Presynaptic calcium/calmodulin-dependent protein kinase II regulates habituation of a simple reflex in adult Drosophila.,” *The Journal of neuroscience : the official journal of the Society for Neuroscience*, vol. 18, no. 21, pp. 8955-64, Nov. 1998.

[37] D. Kamiyama and A. Chiba, “Endogenous activation patterns of Cdc42 GTPase within Drosophila embryos.,” *Science (New York, N.Y.)*, vol. 324, no. 5932, pp. 1338-40, Jun. 2009.

[38] G. B. Gloor, “Gene targeting in Drosophila.,” *Methods in molecular biology (Clifton, N.J.)*, vol. 260, pp. 97-114, Jan. 2004.

[39] K. Zito, D. Parnas, R. D. Fetter, E. Y. Isacoff, and C. S. Goodman, “Watching a synapse grow: noninvasive confocal imaging of synaptic growth in Drosophila.,” *Neuron*, vol. 22, no. 4, pp. 719-29, Apr. 1999.

[40] Y. S. Rong and K. G. Golic, “Gene targeting by homologous recombination in Drosophila,” *Science*, vol. 288, no. 5473, pp. 2013-2018, 2000.

[41] Y. S. Rong and K. G. Golic, “A targeted gene knockout in Drosophila,” *Genetics*, vol. 157, no. 3, pp. 1307-1312, 2001.

[42] Y. S. Rong and K. G. Golic, “The homologous chromosome is an effective template for the repair of mitotic DNA double-strand breaks in Drosophila.,” *Genetics*, vol. 165, no. 4, pp. 1831-42, Dec. 2003.

[43] B. Guan, B. Hartmann, Y. H. Kho, M. Gorczyca, and V. Budnik, "The Drosophila tumor suppressor gene, dlg, is involved in structural plasticity at a glutamatergic synapse," *Curr Biol*, vol. 6, no. 6, pp. 695-706, Jun. 1996.

[44] T. Lahey, M. Gorczyca, X. X. Jia, and V. Budnik, "The Drosophila tumor suppressor gene dlg is required for normal synaptic bouton structure," *Neuron*, vol. 13, no. 4, pp. 823-835, Oct. 1994.

[45] L. Bogdanik et al., "The Drosophila metabotropic glutamate receptor DmGluRA regulates activity-dependent synaptic facilitation and fine synaptic morphology.," *The Journal of neuroscience : the official journal of the Society for Neuroscience*, vol. 24, no. 41, pp. 9105-16, Oct. 2004.

[46] S. B. Marrus, S. L. Portman, M. J. Allen, K. G. Moffat, and A. DiAntonio, "Differential localization of glutamate receptor subunits at the Drosophila neuromuscular junction.," *The Journal of neuroscience : the official journal of the Society for Neuroscience*, vol. 24, no. 6, pp. 1406-15, Feb. 2004.

[47] M. R. Kelley, Y. Xu, D. M. Wilson, and W. A. Deutsch, "Genomic structure and characterization of the Drosophila S3 ribosomal/DNA repair gene and mutant alleles.," *DNA and cell biology*, vol. 19, no. 3, pp. 149-56, Mar. 2000.

[48] K. P. Harris and U. Tepass, "Cdc42 and Par proteins stabilize dynamic adherens junctions in the Drosophila neuroectoderm through regulation of apical endocytosis.," *The Journal of cell biology*, vol. 183, no. 6, pp. 1129-43, Dec. 2008.

[49] A. Hofbauer et al., "The Wuerzburg hybridoma library against Drosophila brain.," *Journal of neurogenetics*, vol. 23, no. 1-2, pp. 78-91, Jan. 2009.

[50] D. A. Wagh et al., "Bruchpilot, a protein with homology to ELKS/CAST, is required for structural integrity and function of synaptic active zones in Drosophila.," *Neuron*, vol. 49, no. 6, pp. 833-44, Mar. 2006.

[51] R. R. Stewart, "Membrane properties of microglial cells isolated from the leech central nervous system," *Proc Biol Sci*, vol. 255, no. 1344, pp. 201-208, 1994.

[52] L. C. Dekkers et al., "Embryonic expression patterns of the Drosophila dystrophin-associated glycoprotein complex orthologs," *Gene Expr Patterns*, vol. 4, no. 2, pp. 153-159, 2004.

[53] L. Y. Jan and Y. N. Jan, "Antibodies to horseradish peroxidase as specific neuronal markers in Drosophila and in grasshopper embryos.," *Proceedings of the National Academy of Sciences of the United States of America*, vol. 79, no. 8, pp. 2700-4, Apr. 1982.

[54] F. Capozzi, C. Luchinat, C. Micheletti, and F. Pontiggia, "Essential dynamics of helices provide a functional classification of EF-hand proteins.," *Journal of proteome research*, vol. 6, no. 11, pp. 4245-55, Nov. 2007.

[55] C. P. Ponting, D. J. Blake, K. E. Davies, J. Kendrick-Jones, and S. J. Winder, "ZZ and TAZ: new putative zinc fingers in dystrophin and other proteins.," *Trends in biochemical sciences*, vol. 21, no. 1, pp. 11-13, Jan. 1996.

[56] V. Budnik et al., "Regulation of synapse structure and function by the Drosophila tumor suppressor gene dlg.," *Neuron*, vol. 17, no. 4, pp. 627-40, Oct. 1996.

[57] D. M. Wilson, W. A. Deutsch, and M. R. Kelley, "Drosophila ribosomal protein S3 contains an activity that cleaves DNA at apurinic/apyrimidinic sites.," *The Journal of biological chemistry*, vol. 269, no. 41, pp. 25359-64, Oct. 1994.

[58] R. S. Zucker and W. G. Regehr, "Short-term synaptic plasticity.," *Annual review of physiology*, vol. 64, pp. 355-405, Jan. 2002.

[59] J. Rohrbough, S. Pinto, R. M. Mihalek, T. Tully, and K. Broadie, “latheo, a Drosophila gene involved in learning, regulates functional synaptic plasticity.,” *Neuron*, vol. 23, no. 1, pp. 55-70, May 1999.

[60] D. J. Sandstrom, “Isoflurane depresses glutamate release by reducing neuronal excitability at the Drosophila neuromuscular junction.,” *The Journal of physiology*, vol. 558, no. 2, pp. 489-502, Jul. 2004.

[61] U. Thomas et al., “Synaptic clustering of the cell adhesion molecule fasciclin II by discs-large and its role in the regulation of presynaptic structure.,” *Neuron*, vol. 19, no. 4, pp. 787-99, Oct. 1997.

[62] M. M. Kucherenko et al., “Genetic modifier screens reveal new components that interact with the Drosophila dystroglycan-dystrophin complex,” *PLoS One*, vol. 3, no. 6, p. e2418, 2008.

[63] C. P. Christoforou, C. E. Greer, B. R. Challoner, D. Charizanos, and R. P. Ray, “The detached locus encodes Drosophila Dystrophin, which acts with other components of the Dystrophin Associated Protein Complex to influence intercellular signalling in developing wing veins,” *Dev Biol*, vol. 313, no. 2, pp. 519-532, 2008.

[64] Y. H. Koh, E. Popova, U. Thomas, L. C. Griffith, and V. Budnik, “Regulation of DLG localization at synapses by CaMKII-dependent phosphorylation,” *Cell*, vol. 98, no. 3, pp. 353-363, 1999.

[65] S. Neuman, M. Kovalio, D. Yaffe, and U. Nudel, “The Drosophila homologue of the dystrophin gene - introns containing promoters are the major contributors to the large size of the gene.,” *FEBS letters*, vol. 579, no. 24, pp. 5365-71, Oct. 2005.

[66] M. L. J. Rees, C.-F. Lien, and D. C. Górecki, “Dystrobrevins in muscle and non-muscle tissues.,” *Neuromuscular disorders : NMD*, vol. 17, no. 2, pp. 123-34, Feb. 2007.

[67] S. V. Böhm and R. G. Roberts, “Expression of members of the dystrophin, dystrobrevin, and dystrotelin superfamily.,” *Critical reviews in eukaryotic gene expression*, vol. 19, no. 2, pp. 89-108, Jan. 2009.

[68] C. F. Lien, C. Vlachouli, D. J. Blake, J. P. Simons, and D. C. Górecki, “Differential spatio-temporal expression of alpha-dystrobrevin-1 during mouse development.,” *Gene expression patterns : GEP*, vol. 4, no. 5, pp. 583-93, Sep. 2004.

[69] R. M. Grady, H. Zhou, J. M. Cunningham, M. D. Henry, K. P. Campbell, and J. R. Sanes, “Maturation and maintenance of the neuromuscular synapse: genetic evidence for roles of the dystrophin--glycoprotein complex,” *Neuron*, vol. 25, no. 2, pp. 279-293, 2000.

[70] J. R. Sanes et al., “Development of the neuromuscular junction: genetic analysis in mice.,” *Journal of physiology, Paris*, vol. 92, no. 3-4, pp. 167-72.

[71] D. Wang, B. B. Kelly, D. E. Albrecht, M. E. Adams, S. C. Froehner, and G. Feng, “Complete deletion of all alpha-dystrobrevin isoforms does not reveal new neuromuscular junction phenotype.,” *Gene expression*, vol. 14, no. 1, pp. 47-57, Jan. 2007.

[72] R. M. Grady, D. F. Wozniak, K. K. Ohlemiller, and J. R. Sanes, “Cerebellar synaptic defects and abnormal motor behavior in mice lacking alpha- and beta-dystrobrevin.,” *The Journal of neuroscience : the official journal of the Society for Neuroscience*, vol. 26, no. 11, pp. 2841-51, Mar. 2006.

[73] K. Gieseler, C. Bessou, and L. Ségalat, “Dystrobrevin- and dystrophin-like mutants display similar phenotypes in the nematode Caenorhabditis elegans.,” *Neurogenetics*, vol. 2, no. 2, pp. 87-90, Apr. 1999.

[74] K. Gieseler et al., “Molecular, genetic and physiological characterisation of dystrobrevin-like (dyb-1) mutants of Caenorhabditis elegans,” *J Mol Biol*, vol. 307, no. 1, pp. 107-117, Mar. 2001.

[75] K. Gieseler, K. Grisoni, M. C. Mariol, L. Segalat, and L. Ségalat, “Overexpression of dystrobrevin delays locomotion defects and muscle degeneration in a dystrophin-deficient Caenorhabditis elegans,” *Neuromuscul Disord*, vol. 12, no. 4, pp. 371-377, May 2002.

## Supplemental Figure

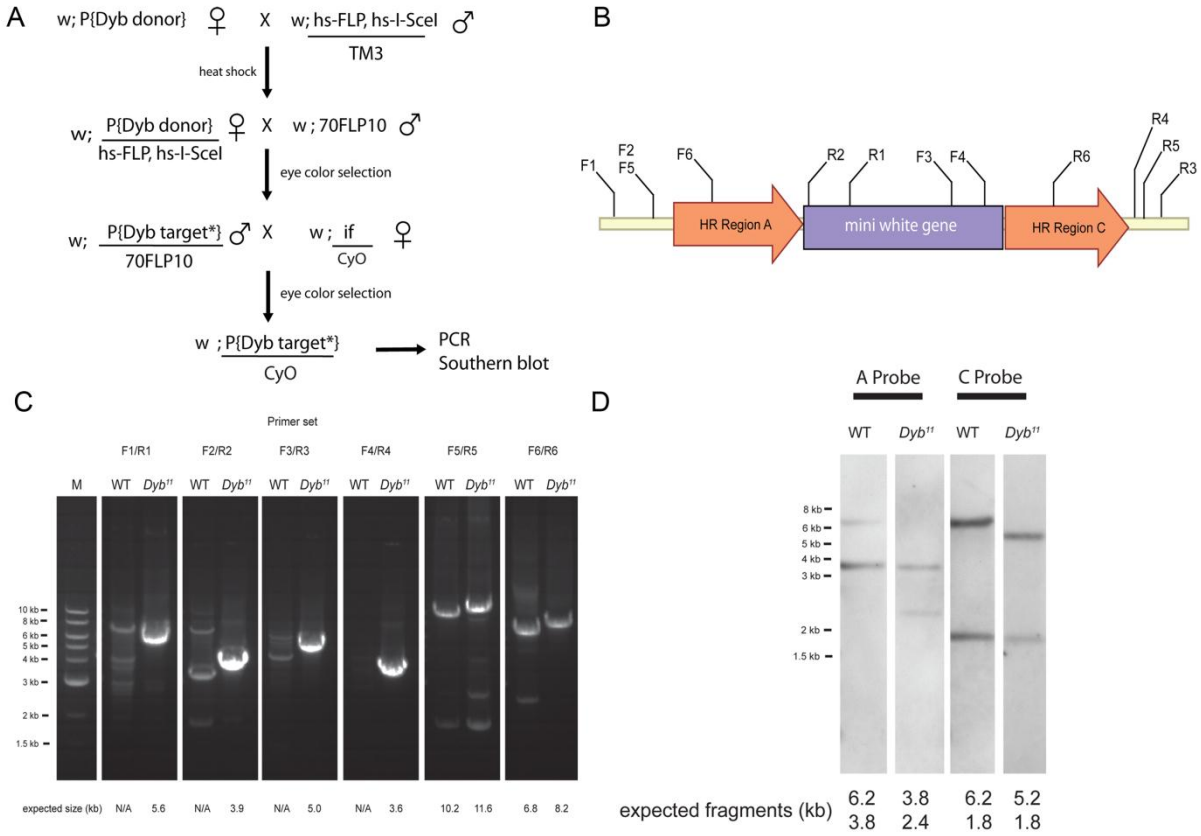


**Supplemental Figure 1. Generation of a *Dyb* mutant.** The crossing scheme for the Dyb gene targeting is shown (**A**). The position of PCR primer sets for the desired targeting events are shown (**B**). The primer sets for the wild type genomic region are shown in **Fig. 1D**. The Dyb gene was replaced by the *white* eye color gene. The molecular structure of the DYB knockout was validated by PCR (**C**) and Southern blotting (**D**).

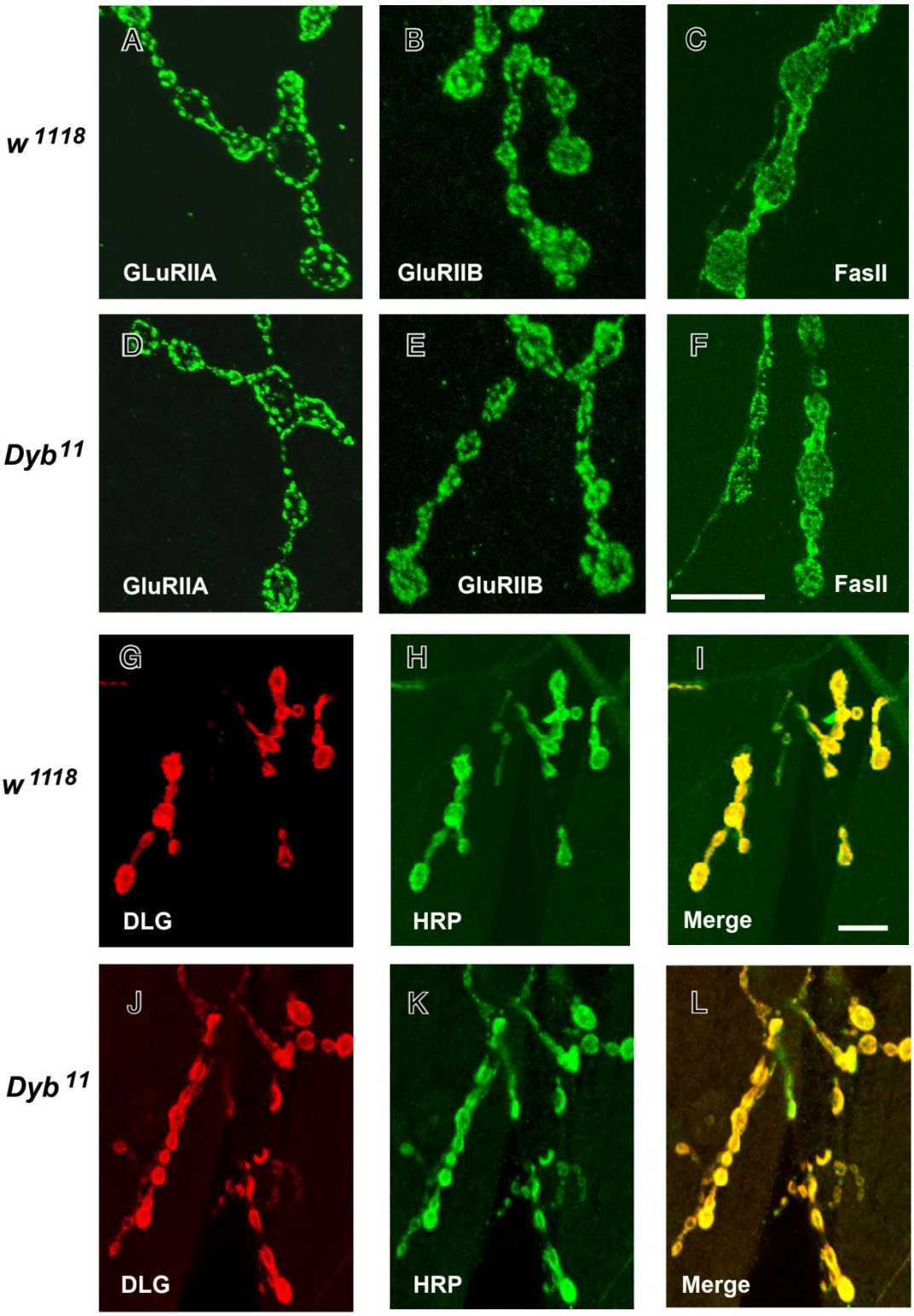


**Supplemental Figure 2. Synaptic morphology and the distribution patterns of the DGluRIIA, DGluRIIB, Fasciclin2 (FasII), Discs-large (DLG) and presynaptic marker stained by anti-HRP are unchanged in *Dyb* mutant.** 3rd instar larval body walls were stained with anti-DGluRIIA (**A** and **D**), anti-DGluRIIB (**B** and **E**), anti-FasII (**C** and **F**), anti-DLG (**G** and **J**) and anti-HRP (**H** and **K**). The merges of anti-DLG and anti-HRP are shown (**I** and **L**). Synapses at muscles 6/7 for wild type controls (**A**, **B**, **C**, **G**, **H** and **I**) and *Dyb* mutants (**D**, **E**, **F**, **J**, **K** and **L**) are shown.

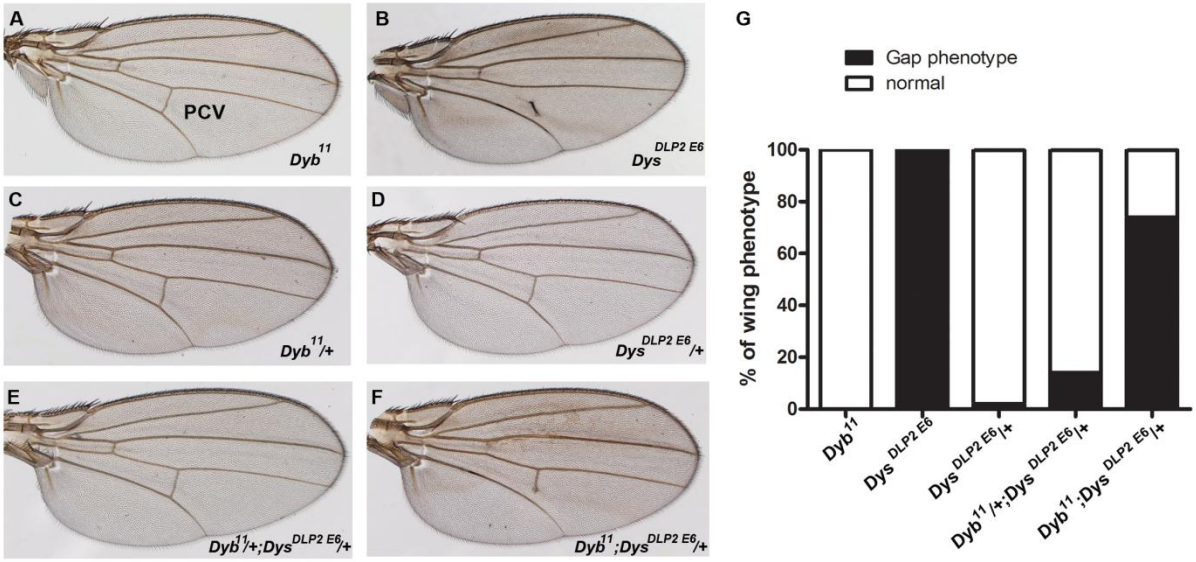


**Supplemental Figure 3. *Dyb* interacts genetically with Dystrophin during crossvein formation in *Drosophila* wings.** Wing of homozygous $Dyb^{11}$ (**A**), heterozygous $Dyb^{11}$/+ (**C**) and heterozygous $Dys^{DLP2\ E6}$/+ (**D**) exhibit a wild type posterior crossvein (PCV). The heterozygous double mutant $Dyb^{11}$/+; $Dys^{DLP2\ E6}$/+ (**E**) also show normal wing vein formation. Homozygosity for $Dyb^{11}$ with simultaneous heterozygosity for $Dys^{DLP2\ E6}$ results in PCV with a gap phenotype which is also observed in animals homozygous for $Dys^{DLP2\ E6}$ (**B**). This result indicates the existence of a genetic interaction between *Dystrophin* and *Dyb* during wing vein formation. Quantitation of this phenotype is shown (**G**).

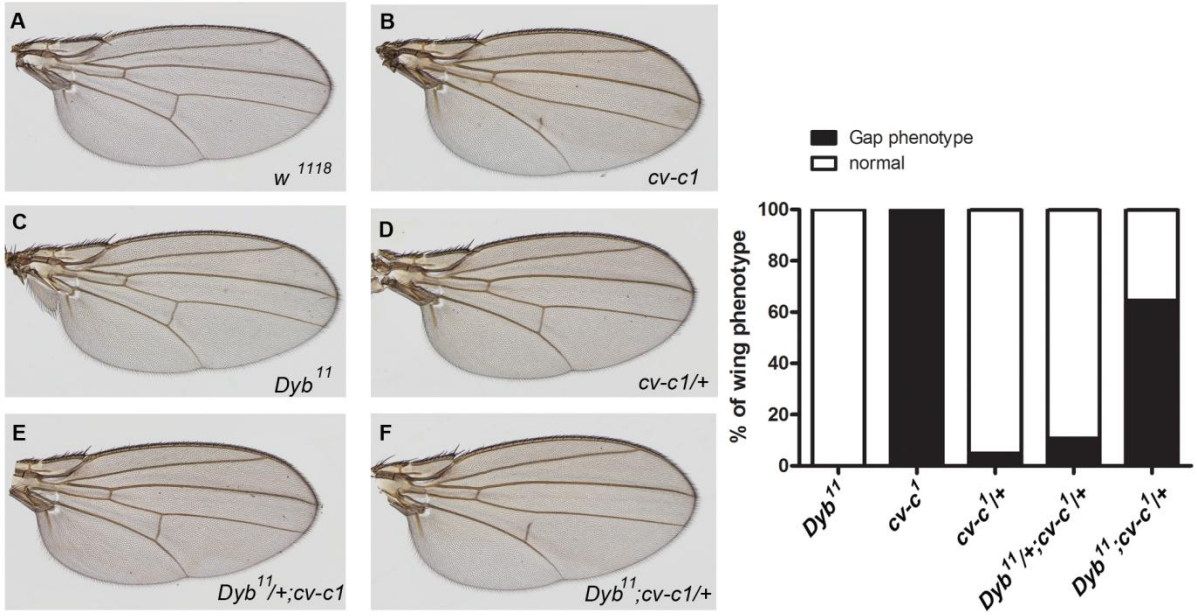


**Supplemental Figure 4. Dystrobrevin interacts genetically with RhoGap *cv-c* to stabilize crossvein formation in *Drosophila* wings.** Wing of homozygous $Dyb^{11}$ (**A**), heterozygous $Dyb^{11}$/+ (**C**) and heterozygous $cv\text{-}c^{1}$/+ (**D**) exhibit a wild type posterior crossvein (PCV). The heterozygous double mutant $Dyb^{11}$/+; $cv\text{-}c^{1}$/+ (**E**) also show normal wing vein formation. The homozygous of $Dyb^{11}$ with heterozygous $Dys^{DLP2\ E6}$/+ [$Dyb^{11}$; $cv\text{-}c^{1}$/+] (**F**) only has uncompleted formed PCV (gap phenotype). This gap phenotype is also observed in homozygous $cv\text{-}c^{1}$ (**B**). This result indicates a genetic interaction between DYB and RhoGap $cv\text{-}c^{1}$ in the wing. Histogram (**G**) shows percentage of wing phenotype of genotypes indicated in the pictures.

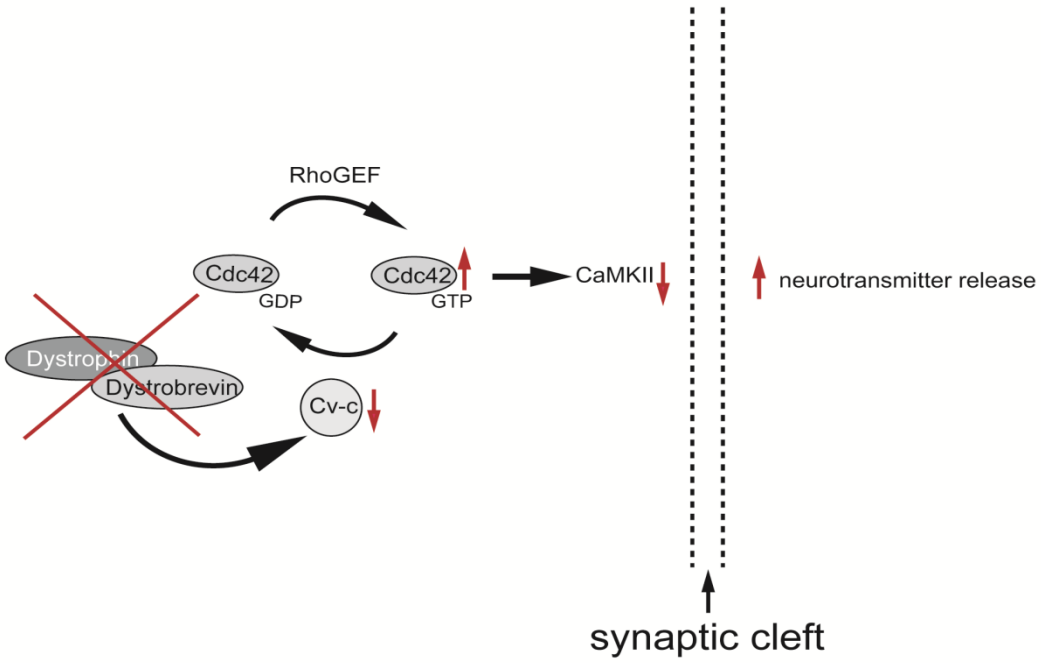


**Supplemental Figure 5. A schematic model for the regulation of presynaptic neurotransmitter release by a postsynaptic Dystrophin/DYB complex at the *Drosophila* NMJ.** Models for the Dystrophin-deficient or the *Dyb* mutant NMJs are presented. Dystrophin and DYB somehow maintains wild type activity levels of the Rho-GAP CV-C whose inactivation of the Rho-GTPase, CDC42, is counterbalanced by an unknown RhoGEF. The absence of Dystrophin resulted in mislocalized of DYB leads to decreased activity of CV-C which, in turn, leads to increased levels of active GTP-bound CDC42. Active CDC42 subsequently decrease level of CaMKII leading to an alteration in a retrograde message(s) which transmits a signal across the synaptic cleft leading to increased presynaptic neurotransmitter release. At present, we do not know if the absence of Dystrophin and DYB result in increased or decreased retrograde signaling. Such signals may be transduced by soluble factors secreted across the synaptic cleft or by trans-synaptic protein interactions.

**Supplemental table 1. Average electrophysiological data including fmEJPs, mEJPs, EJPS and QC of all genotypes**

**Raw data of Fig.4 and 5**

| Genotype | | fmEJP | mEJP | EJP | QC |
|---|---|---|---|---|---|
| $w^{1118}$ | Mean | 2.66 | 0.74 | 25.18 | 47.29 |
| | Std.Error of Mean* | 0.75 | 0.05 | 1.28 | 3.77 |
| | N# | 14 | 14 | 14 | 14 |
| $Dyb^{11}$ | Mean | 3.21 | 0.71 | 34.58 | 71.48 |
| | Std.Error of Mean | 0.36 | 0.04 | 0.79 | 6.60 |
| | N | 17 | 17 | 17 | 17 |
| $Dyb^{11}$/+ | Mean | 2.72 | 0.69 | 33.31 | 68.75 |
| | Std.Error of Mean | 0.20 | 0.05 | 1.4 | 3.94 |
| | N | 10 | 10 | 10 | 10 |
| Df(2R)Exel6061/Df(2R)$achi^4$ *Dyb* deficiency | Mean | 3.44 | 0.72 | 32.30 | 63.27 |
| | Std.Error of Mean | 0.51 | 0.07 | 1.85 | 3.43 |
| | N | 5 | 5 | 5 | 5 |
| OK6-GAL4/+ | Mean | 3.69 | 0.82 | 26.83 | 43.02 |
| | Std.Error of Mean | 0.42 | 0.02 | 0.94 | 2.18 |
| | N | 20 | 20 | 20 | 20 |
| 24B-GAL4/+ | Mean | 2.26 | 0.77 | 23.89 | 40.81 |
| | Std.Error of Mean | 0.30 | 0.06 | 1.13 | 1.98 |
| | N | 11 | 11 | 11 | 11 |
| mhc-GAL4/+ | Mean | 2.74 | 0.79 | 25.82 | 39.88 |
| | Std.Error of Mean | 0.55 | 0.07 | 1.34 | 3.28 |
| | N | 6 | 6 | 6 | 6 |
| $Dyb^{11}$, OK6-GAL4/+ | Mean | 2.44 | 0.73 | 34.32 | 67.73 |
| | Std.Error of Mean | 0.29 | 0.05 | 1.27 | 4.13 |
| | N | 10 | 10 | 10 | 10 |
| $Dyb^{11}$/+; 24B-GAL4/+ | Mean | 3.06 | 0.88 | 34.71 | 55.42 |
| | Std.Error of Mean | 0.57 | 0.05 | 1.27 | 2.23 |
| | N | 5 | 5 | 5 | 5 |
| $Dyb^{11}$,OK6-GAL4/+; UAS-*Dyb*/+ | Mean | 4.21 | 0.75 | 35.99 | 69.35 |
| | Std.Error of Mean | 0.82 | 0.06 | 1.9 | 3.93 |
| | N | 10 | 10 | 10 | 10 |
| $Dyb^{11}$; UAS-*Dyb*/24B-GAL4 | Mean | 3.38 | 0.85 | 25.88 | 39.86 |
| | Std.Error of Mean | 0.54 | 0.05 | 1.14 | 2.6 |
| | N | 8 | 8 | 8 | 8 |
| $Dyb^{11}$/+; mhc-GAL4/+ | Mean | 3.13 | 0.78 | 33.39 | 60.21 |
| | Std.Error of Mean | 0.44 | 0.06 | 1.15 | 3.35 |
| | N | 7 | 7 | 7 | 7 |

* Standard error of mean
\# Number of lavae

**Raw data of Fig.6 Dyb –shakker**

| Genotype | | fmEJP | mEJP | EJP | QC |
|---|---|---|---|---|---|
| $w^{1118}$ | Mean | 3.32 | 0.66 | 23.47 | 44.95 |
| | Std.Error of Mean | 1.52 | 0.06 | 1.86 | 3.06 |
| | N | 7 | 7 | 7 | 7 |
| $w^{1118}$; Df(3R)Exel6184 Df(*Dys*) | Mean | 1.87 | 0.78 | 31.68 | 56.36 |
| | Std.Error of Mean | 0.06 | 0.05 | 1.68 | 3.19 |
| | N | 7 | 7 | 7 | 7 |
| PTWMDyb-sh/OK6-GAL4; Df(*Dys*) | Mean | 1.88 | 0.88 | 33.43 | 53.67 |
| | Std.Error of Mean | 0.27 | 0.07 | 1.39 | 4.08 |
| | N | 5 | 5 | 5 | 5 |
| PTWMDyb-sh/G14-GAL4; Df(*Dys*) | Mean | 2.85 | 1.12 | 27.04 | 32.84 |
| | Std.Error of Mean | 0.21 | 0.1 | 1.65 | 3.23 |
| | N | 6 | 6 | 6 | 6 |

**Raw data of Fig.7 and Fig.8 Dyb and $Cdc42^4$ , Dyb and CaMKII**

| Genotype | | fmEJP | mEJP | EJP | QC |
|---|---|---|---|---|---|
| $w^{1118}$ | Mean | 2.66 | 0.74 | 25.18 | 47.29 |
| | Std.Error of Mean | 0.75 | 0.05 | 1.28 | 3.77 |
| | N | 14 | 14 | 14 | 14 |
| $Dyb^{11}$/+ | Mean | 2.72 | 0.69 | 33.31 | 68.75 |
| | Std.Error of Mean | 0.20 | 0.05 | 1.4 | 3.94 |
| | N | 10 | 10 | 10 | 10 |
| $Dyb^{11}$/+;mhc-GAL4/+ | Mean | 3.13 | 0.78 | 33.39 | 60.21 |
| | Std.Error of Mean | 0.44 | 0.06 | 1.15 | 3.35 |
| | N | 7 | 7 | 7 | 7 |
| $Dyb^{11}/Cdc42^4$ | Mean | 3.00 | 0.93 | 26.25 | 37.67 |
| | Std.Error of Mean | 0.16 | 0.09 | 1.12 | 2.71 |
| | N | 6 | 6 | 6 | 6 |
| $Dyb^{11}$/+;RNAiCdc42/mhc-GAL4 | Mean | 5.17 | 0.91 | 25.96 | 36.24 |
| | Std.Error of Mean | 0.53 | 0.06 | 2.62 | 3.35 |
| | N | 5 | 5 | 5 | 5 |
| $Dyb^{11}$/+;UAS-*CaMKT287D*/24B-GAL4 | Mean | 3.77 | 0.82 | 26.8 | 43.3 |
| | Std.Error of Mean | 0.61 | 0.07 | 0.95 | 3.39 |
| | N | 7 | 7 | 7 | 7 |
| $Dyb^{11}$/+;UAS-*CaMKT287D*/mhc-GAL4 | Mean | 5.13 | 1.0 | 28.22 | 37.31 |
| | Std.Error of Mean | 0.64 | 0.07 | 0.74 | 2.67 |
| | N | 6 | 6 | 6 | 6 |
| $Dyb^{11}$/+;UAS-*CaMKT287A*/24B-GAL4 | Mean | 2.82 | 0.76 | 31.37 | 56.24 |
| | Std.Error of Mean | 0.48 | 0.06 | 2.84 | 2.62 |
| | N | 5 | 5 | 5 | 5 |
| $Dyb^{11}$/+;UAS-*CaMKT287A*/mhc-GAL4 | Mean | 5.23 | 0.75 | 33.89 | 63.81 |
| | Std.Error of Mean | 0.59 | 0.05 | 1.29 | 2.35 |
| | N | 6 | 6 | 6 | 6 |

**Raw data of Fig.9 and Fig. 10 CaMK is working downstream of Cdc42**

| Genotype | | fmEJP | mEJP | EJP | QC |
|---|---|---|---|---|---|
| $w^{1118}$ | Mean | 2.34 | 0.71 | 21.62 | 39.75 |
| | Std.Error of Mean | 0.28 | 0.04 | 1.12 | 2.6 |
| | N | 5 | 5 | 5 | 5 |
| OK6-GAL4 | Mean | 3.45 | 0.83 | 27.25 | 43.51 |
| | Std.Error of Mean | 0.55 | 0.02 | 1.16 | 2.65 |
| | N | 15 | 15 | 15 | 15 |
| mhc-GAL4 | Mean | 2.64 | 0.88 | 26.01 | 39.17 |
| | Std.Error of Mean | 0.45 | 0.77 | 1.02 | 2.49 |
| | N | 8 | 8 | 8 | 8 |
| UAS-cdc42/+ | Mean | 2.42 | 0.69 | 24.33 | 45.2 |
| | Std.Error of Mean | 0.25 | 0.03 | 0.78 | 3.2 |
| | N | 6 | 6 | 6 | 6 |
| UAS-cdc42/OK6-GAL4 | Mean | 3.72 | 0.75 | 26.12 | 45.48 |
| | Std.Error of Mean | 0.63 | 0.03 | 0.84 | 3.06 |
| | N | 6 | 6 | 6 | 6 |
| UAS-cdc42/mhc-GAL4 | Mean | 2.45 | 0.72 | 31.59 | 61.75 |
| | Std.Error of Mean | 0.53 | 0.11 | 2.36 | 3.73 |
| | N | 6 | 6 | 6 | 6 |
| UAS-cdc42/+; UAS-mCD8GFP/mhc-GAL4 | Mean | 3.09 | 0.7 | 29.86 | 57 |
| | Std.Error of Mean | 0.47 | 0.05 | 1.53 | 3.16 |
| | N | 8 | 8 | 8 | 8 |
| UAS-cdc42/+; UAS-*CaMKT287D*/mhc-GAL4 | Mean | 3.25 | 0.8 | 23.96 | 37.56 |
| | Std.Error of Mean | 0.48 | 0.04 | 1.43 | 2.16 |
| | N | 9 | 9 | 9 | 9 |
| $Cdc42^{4}$/+ | Mean | 2.79 | 0.86 | 25.71 | 40.52 |
| | Std.Error of Mean | 0.5 | 0.08 | 1.25 | 4.63 |
| | N | 6 | 6 | 6 | 6 |
| UAS-Ala/mhc-GAL4 | Mean | 1.3 | 0.64 | 28.42 | 57.91 |
| | Std.Error of Mean | 0.09 | 0.04 | 0.81 | 2.3 |
| | N | 5 | 5 | 5 | 5 |
| $Cdc42^{4}$/+; UAS-Ala/mhc-GAL4 | Mean | 2.63 | 0.74 | 32.44 | 61.07 |
| | Std.Error of Mean | 0.24 | 0.04 | 0.81 | 2.8 |
| | N | 5 | 5 | 5 | 5 |